2002

Analysis of bolted flange connections under tensile loading.

Yail. Kim
University of Windsor

ANALYSIS OF BOLTED FLANGE CONNECTIONS UNDER TENSILE LOADING

BY

YAIL KIM

A Thesis
Submitted to the Faculty of Graduate Studies and Research through
The Department of Civil and Environmental Engineering
in Partial Fulfillment of the Requirements for the
Degree of Master of Applied Science at the
University of Windsor

Windsor, Ontario, Canada
2002

I hereby declare that I am the sole author of this document.

I authorize the University of Windsor to lend this document to other institutions or individuals for the purpose of scholarly research

yail J. Kim

I further authorize the university of Windsor to reproduce the document by photocopying or by other means, in total or part, at the request of other institutions or individuals for the purpose of scholarly research

yail J. Kim

The UNIVERSITY OF WINDSOR requires the signature of all persons using or photocopying this document.

Please sign below and give address and date.

ABSTRACT

This thesis aims to analyze general behavior and characteristics of bolted flange connections under tensile loading conditions. Twelve specimens, in total, were used in the experimental work to estimate the effect of the external load to the bolts and flange separation. Based on these data, several phenomena were analyzed such as prying action, relation between the external load and bolt force, and gap development.

After collecting the results mentioned above, they were compared with well-known T-stub connections to verify the applicability of a rounded bar connection. In order to arrive at a better understanding of the bolted connection, the finite element analysis was performed employing ABAQUS.

Finally, a systematic and step-by-step design approach for the bolted rounded bar connection is suggested and an automatic design program has been developed using MATLAB.

Standing on the shoulder of a giant.

ACKNOWLEDGEMENT

Thanks to

Issac Newton, Christian Otto Mohr, Du Perron Rene Descartes, Leonhard Euler, Thomas Young, Simon-Denis Poisson, Robert Hooke, Galileo Galilei

Dr. Sungchul Lee, Dr. Changsik Min, Dr.Fouzi Ghrib, Dr. Nihar Biswas, Dr.B. Budkowska, Dr.N.Zamani, Ms. JoAnn Grondin, Mr. Richard Clark, Ms. Lihong Shen, Mr. Yongcong Ding

Academic Writing Center in the University of Windsor

Electronics Research Inc.

Dongguk University, University of Windsor

Families in Seoul, S. Korea

Special thanks to Dr. Murty K.S. Madugula

Very special thanks to Habin Kim , new one and Seohoung Kim

TABLE OF CONTENTS

III. ANALYSIS OF BOLTED THE FLANGE CONNECTION

IV. ANALYTICAL MODELING

V. DESIGN RECOMMENDATIONS

LIST OF TABLES

LIST OF FIGURES

NOTATION

A = Cross sectional area

A_b = Nominal bolt area

A_s = Stress area

B, B_u, F, F_B = Bolt force

B_{min} = Minimum bolt force

ΔB = Increase of bolt force

B_{all} = Allowable bolt force

C = Connection capacity

C_J = Contact force of a joint

D = Nominal diameter of a bolt

$\{D\}$ = Displacement vector

d = Diameter of a rod

D_B = Flat length on the bolt head

D_i = Inside of diameter of a load cell

D_o = Outside diameter of a load cell

E = Young's modulus

F = Sample number in group 2

F.S. = Factor of safety

ΔF_{EI} = Elastic interaction loss of preload

ΔF_m = Embedment loss of preload

F_{pr}, F_{pa} = Preload of a bolt

F_y, σ_y = Yield strength

H = Length of a bolt head

h = height of a load cell

[K] = Structural stiffness matrix

K_B = Stiffness of a bolt

K_J = Stiffness of a joint

L = Length of bolt shank

L_B = Length of bolt shank except for thread

ΔL_B = Change in length of the grip length portion of a loose bolt

ΔL_J = Change in thickness of the joint members, before assembly

L_L = Grip length

L_T = Length of thread

L_t = Total length of a bolt

N = Length of a nut

n = Loading plane factor, number of bolts

{P} = Applied load vector

p = Bolt pitch

P_f = Load applied per bolt

Q = Prying force

R_n = Nominal strength

S = Sample number in group 1

s = Scatter factor

T, L_X = External load applied

t = Flange thickness

T_H = Thickness of a bolt head

T_N = Thickness of a nut

T_r = Factored tensile resistance of a bolt

ε = Strain

Φ_{en} = Load factor for the joint

Φ = Load and resistance factor

σ_u = Ultimate strength

Ψ = Load factor

CHAPTER I

INTRODUCTION

1.1 General

Because of the limit of structural members' length, connections between the members are inevitable. Several kinds of connection methods are used in current industry such as bolting, riveting, and welding. Out of these various methods, bolting is a very general and useful means to connect structural members because of a number of benefits such as:

(1) Reducing risks in the construction field compared with riveting and welding in terms of problems caused by fire.

(2) Being easy to modify when the connection does not function properly.

(3) Being convenient to connect in the construction field. There is no need to prepare special equipment such as a compressor.

(4) Being possible to construct economically.

Therefore, the usage of bolted joints has been increasing not only in large structures such as bridges, but also relatively small structures such as communication towers.

In order to understand the phenomenon of the bolting method, solid round leg members of a communication tower can provide a good example since these are not part of a relatively large-scale structure, furthermore they are used through out countries such as

Canada and the U.S.A. Hence, the study of bolted connections is essential.

1.2 Need for Research

As mentioned previously, this work aims to study and analyze the behavior of bolted connections between solid round bars. There must be several connection methods and various kinds of loading conditions. Of those, bolted flanges under tensile loading will be studied. Much is known about the bolted flanges in the field of T-stub connections already. Solid round bars, however, have not been studied intensively. Consequently, even though the use of a solid round bar connection is also as common as that of the T-stubs, few things to date are known about the solid round bar connection. Therefore, intensive study is needed about this matter and applicability of T-stub-behavior to a solid round bar connection must be investigated as well.

(a) T-stub connection (b) Round flange connection

Fig.1.1 Bolted connection

<T-stub source: www.ce.gatech.edu/~sac>

In order to improve the understanding of the bolted connection, a finite element analysis was performed. Many researchers have employed the finite element method for the purpose of analysis nowadays. The finite element analysis must be the most powerful and reliable tool than any other methods developed so far. And many of them accepted 2-D modeling methods since these are computationally economical, less laborious and convenient to access while providing relatively reliable results. However, an approximate modeling is usually performed when it comes to the 2-D modeling. Sherbourne & Bahaari (1996), moreover, have developed 3-D models for T-stub connections already [11]. However, analytical models for a solid round bar connection have not yet been reported. For this thesis, ABAQUS code was used.

In addition, this study will enhance the understanding of bolted round flange connections and play an important role as part of design and analysis of the whole communication tower as well.

1.3 Objectives of Research

The main objectives of the present research work are listed below

(1) To analyze the relation between prying action and the applied external tensile load.

(2) To analyze the effect of the external tensile load to bolt force.

(3) To analyze the relation between separation of the flanges and the external tensile load.

(4) To confirm the application of well-known T-stub design methods to solid round bar

connections.

(5) To enhance general understanding of bolted connections through analytical modeling.

(6) To compare the general behavior of the round bar connection with the T-stub connection.

(7) To suggest design recommendations for a round flange connection.

(8) To develop a brief and easy automatic design program for the user's convenience.

1.4 Contents and Arrangement of the Thesis

Chapter I was already written to show the need for this research work. In order to contribute to an understanding of the problems and enhance comprehension of the bolted connections. the available literature will be reviewed in Chapter II. Chapter III deals with the experimental work in detail and the analyses are reviewed. In Chapter IV. analytical models are developed. Design recommendations for a round flange connection are suggested in Chapter V and the following Chapter VI shows how to access an automatic design program. Finally, Chapter VII summarizes this document and suggests conclusions based on the current research and makes recommendations for future study.

CHAPTER II

LITERATURE REVIEW

2.1 General

2.1.1 Basics of bolted connections

Bolted joints between structural members can be categorized depending on the direction of applied external loads. One is a tensile joint when the external load is applied in parallel direction of the fastener's axis. The other is a shear joint when the applied load is operated in perpendicular direction. Sometimes, one more case happens when the joints undergo mixed loading conditions.

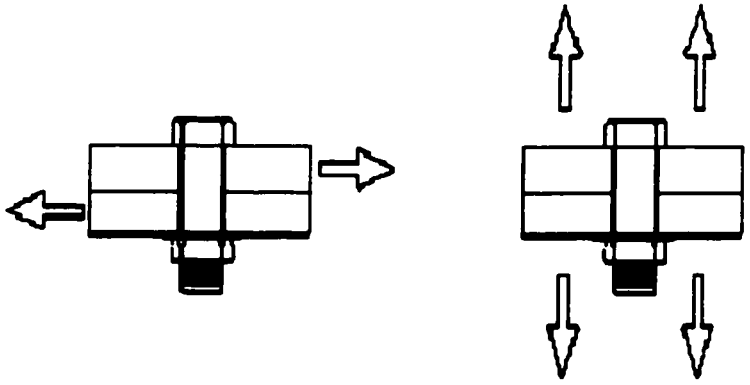

(a) Shear joint (b) Tensile joint

Fig. 2.1 Shear joint and tensile joint

2.1.2 Tensile and shear joints

The role of a bolt in tensile joints is to prevent separation or leaking of the joints. Initial preload or clamping force is applied through the assembly process. In addition to this, the given preload must be sufficient to resist self-loosening caused when the joints are exposed to thermal effect, vibration, impact and corrosion. Kulak et al. (1987) suggested that there are two important things to keep in mind when designing tensile joints "*(1) The bolt is a mechanism for creating and maintaining a force, the clamping force between joint members. (2) The behavior and life of the bolted joint depend very much on the magnitude and stability of that clamping force*"[7]

When it comes to shear joints, the bolts must be strong enough to withstand slipping and tearing apart in the slip direction. Of course, the clamping force or initial preload must be needed to prevent such behaviors by providing frictional face on the surface of the joints.

To control this important preload, during assembly procedure, preload control can be performed by monitoring strain gages and using some equipment such as a bolt tensioner (refer to 2.5.2).

2.1.3 General behavior of bolt property under tensile loading

A bolt is generally made of steel: carbon steel or alloy steel. Like other general steel material, a bolt shows typical force vs. elongation curve (Fig.2.2). Understanding this basic curve is extremely crucial in order to comprehend general behavior under tensile

loading. As is already known, most design codes are within the elastic region, thus no permanent deformation is permitted. The *limit states design method* can be used by considering plastic behavior of the bolts. The real situation, however, has numerous variables; so it is very hard to predict the behavior exactly. Therefore, the elastic design is more popular since it is more conservative.

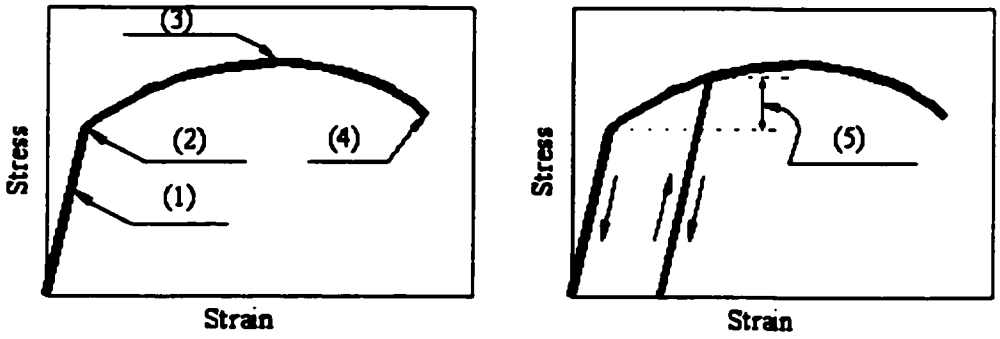

(a) general (b) plastic behavior

(1) elastic range, (2) yield stress, (3) ultimate stress, (4) breaking, (5) strain hardening

Fig.2.2 Typical behavior of a bolt under tensile loading

2.1.4 Modes of failure

Smistakidis et al. (1997) suggested that three different types of failure exist in T-stub connections. (1) Complete flange yielding (Mode I): two plastic hinges are created through just around the bolt-hole and the boundary of the web. (2) Bolt failure with flange yielding (Mode II): flange yielding occurs around the web and the bolt also yields simultaneously. (3) Complete bolt failure (Mode III): when stiffness of the flange is much

larger than that of the bolts, only bolt failure occurs [13].

2.2 Connections under Tensile Loading

2.2.1 Relations between deflection and force

Bickford (1981) suggested that the applied force is proportional to its elongation [1] (refer to Fig.2.3), that is,

$$\Delta F_B = K_B * \Delta_B \quad \text{and} \quad \Delta C_J = K_J * \Delta_J$$

where ΔF_B =Change of bolt force

K_B =Stiffness of the bolt

Δ_B = Change of bolt length

ΔC_J =Change of contact force of the joints

K_J =Stiffness of the joints

Δ_J = Change of the thickness of the joints

Therefore, the relation between them can be expressed. After assembly, the state of the bolt and the flange is shown in Fig.2.3 (a). After loading, the force of the bolt increases and the clamping force or *the joint force* decreases (refer to Fig.2.3 (b)).

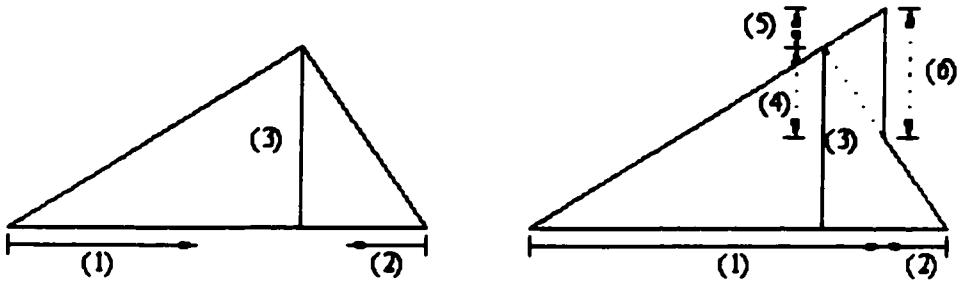

(a) initial state (b) after external loading

(1) change of bolt length, (2) change of joint length, (3) preload, (4) change of joint force (5) change of bolt force, (6) external load

Fig. 2.3 Relation between deflection and forces

2.2.2 The joint diagram

For this thesis, one more convenient joint diagram introduced by Kulak et al. (1981) is used, and the use of this diagram is more common than the former one [7]. The reason that this joint diagram is selected is prying action can be expressed more clearly.

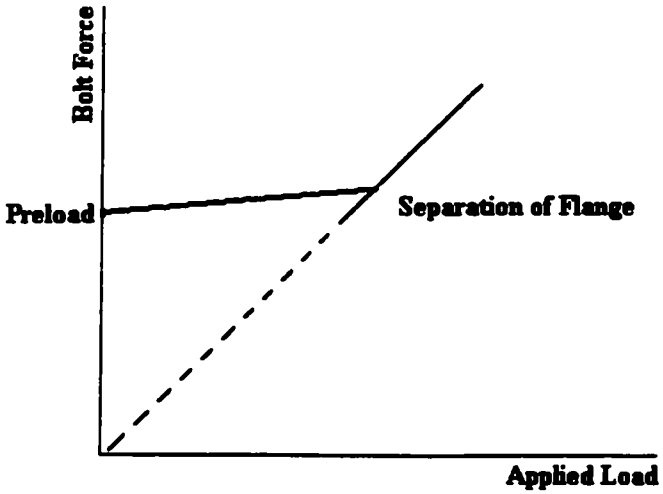

Fig. 2.4 Joint diagram

2.3 Prying Action

2.3.1 Definition of prying action

As external forces are applied, the contact force or *the joint force* of the flange is reduced (refer to Fig.2.3). But, here, one special phenomenon is shown. Additional force on the tip of the flange occurs until complete-joint-separation. This phenomenon is called *prying action* or *prying force* (refer to Fig.2.5). This prying action largely depends on the stiffness and the thickness of the flange. This force is almost impossible to detect during experiments. Therefore, exact investigation is very hard. In general, this force can be expressed as

$$B = T + Q$$

where, B: Total bolt force

T: External force

Q: Total prying force

Hence, it is obvious that the prying action increases the bolt force and this force must be considered in the design or analysis of bolted connections.

2.3.2 Suggested formulae for bolt force calculation

As mentioned previously, investigating the exact prying force is almost impossible. In addition, the real prying force is shown as non-linear (refer to Fig.2.6). Kulak et al. (1987) suggested that the guide line for the bolt side can be drawn 5 ~ 10% increment of the external load until it meets 1:1 line [7].

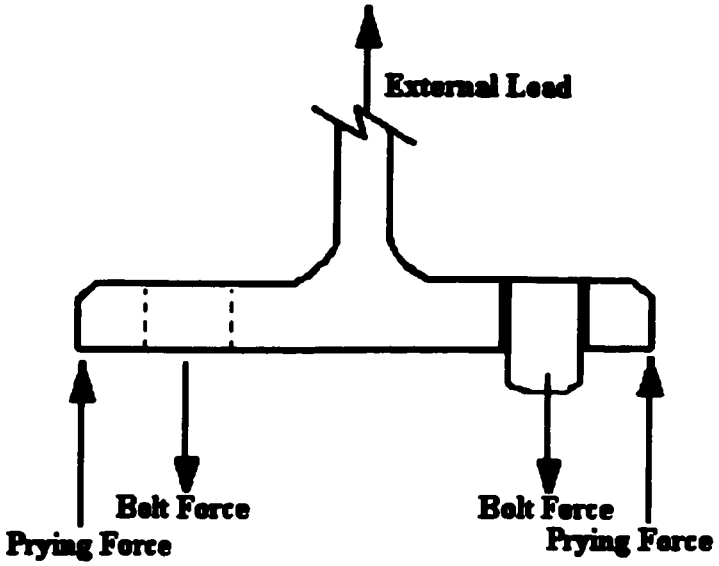

Fig.2.5 General diagram of prying action

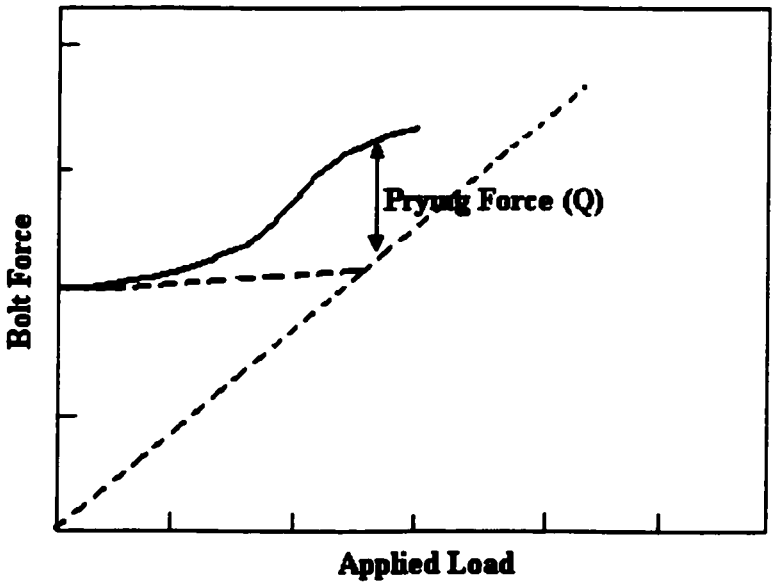

Fig.2.6 Non-linear prying action

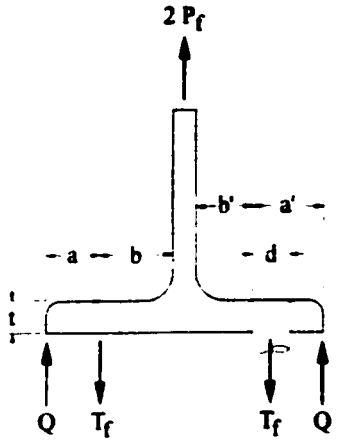

$$B = \left[1 + \frac{\delta\alpha}{(1+\delta\alpha)}\frac{b}{a}\right]T \qquad (2\text{-}1)$$

where,

B = Bolt force (kN)

T = Applied external load (kN)

δ = Ratio of net to gross flange area along a longitudinal line of bolts

α = Ratio of sagging moment at bolt line to hogging moment at stem of tee

a = Distance from bolt line to edge of tee flange, not more than 1.25b (mm)

b = Distance from bolt line (gauge line) to face of tee stem (mm)

$$F_B = (1 + s)\,F_{pa} - \Delta F_m - \Delta F_{EI} + \Phi_{en} L_X \pm \Phi_{en} K_J''(\Delta L_J - \Delta L_B) \qquad (2\text{-}2)$$

where,

F_B = Bolt force (N)

s = Assembly scatter factor (0~1)

F_{pa} = Average or target assembly preload (N)

ΔF_m = Change in preload created by embedment relaxation (N)

ΔF_{EI} = Reduction in average, initial, assembly preload caused by elastic interactions (N)

Φ_{cn} = Load factor for the joint whose stiffness is K_J"

L_X = External load applied (N)

K_J" = Stiffness of a joint in which both the axes of the bolts and the line of application of a tensile force are offset from the axis of gyration of the joint, and in which the tensile load is applied along loading planes located within the joint members (N/m).

ΔL_J = Change in thickness of the joint members, before assembly, if exposed to the same Δt (m).

ΔL_B = Change in length of the grip length portion of a loose bolt created by a change of Δt (m).

Of many equations, in the current industry Eq.2-1 (from CISC or *Canadian Institute of Steel Construction*) and Eq.2-2 (from VDI or *German Engineering Society*) are the most popular to calculate the bolt force in T-stub equivalent connections. These equations will be discussed in Chapter III and Appendix B in detail.

2.4 Loading Plane Theory

The exact place the external tensile load is applied is not known in the joint material. However, an exact location is needed to figure out detailed stresses in the joint, for instance, by the finite element analysis. Bickford (1981) developed a theory to describe this loading place called a *loading plane* [1]. This plane is parallel to the joint interface and located somewhere in the joint. The external tensile loading is applied on this plane. It is assumed that the place between a loading plane and the interface is independent of the loading. Bickford (1981) suggested a ratio between the thickness of the whole joint and that of the loading part called *loading plane factor* (n) [1].

$$n = \frac{t_{all}}{t_{unload}}$$

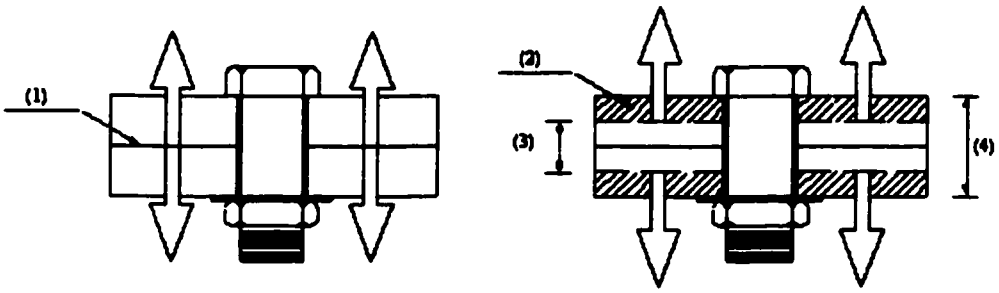

(a)interface-loading case (b)loading-plane loading case

(1) interface plane, (2)loading plane, (3) t_{unload}, (4) t_{all}

Fig.2.7 Loading plane

This factor is required to calculate bolt forces. Bickford (1995) recommended 0.5 for

this value. He also commented that this location was difficult to find and the assumed value, n=0.5, was accurate enough for virtually all applications [1].

2.5 Structural Fastener

2.5.1 Definition and basics

In order to understand structural connections, structural fasteners must be studied. According to ASTM, several types of bolts are defined.

(1) ASTM A307 – Low carbon steel bolts and other fasteners.

(2) ASTM A325 – High strength medium carbon steel bolts.

(3) ASTM A490 – Alloy steel bolts.

(4) ASTM A 449, A354 – Special types of high strength bolts such as interference body bolts, swedge bolts, etc.

In general, A325 and A490 are commonly used. Bolt type and manufacture's identification mark must be marked on the head of every bolt. For the A325 bolt, the minimum tensile strength for up to 1 inch diameter is 120 ksi and 105 ksi for 1 1/8 to 1 1/2 inch. However, for the A490 bolt, 150 ksi is used for every type. For defining the elastic range, 0.2% offset method is used. However, ASTM recommends a direct tension test for the full size of bolts to decide actual material properties, and the ultimate strength varies depending on whether it was torqued or not. In torqued bolts, usually 5-25%, average 15%, reduction was reported in both A325 and A490 (Kulak et al. 1987) [7]. On the basis of this ultimate strength, the

minimum fastener tensions are regulated, for instance, 19 kips or 85 kN for a 5/8 inch A325 bolt.

2.5.2 Assembly

One of the most important things in bolt assembly is preload control. When the high strength bolt was on the market, torque control was the primary method. But assembly in the field had a number of variables such as thread conditions, assembler's experience, lubrication, etc. The next generation was the calibrated wrench method. Preload was controlled by strain monitoring using a direct tension indicator in this method but soon problems were reported like the former method. To overcome these problems, the modified turn-of-nut method was devised. In this method, the bolt was tightened by turning the nut by, for example, one-half or one-third turn of the nut from the snug tight condition.

CHAPTER III

ANALYSIS OF THE BOLTED FLANGE CONNECTION

3.1 General

In order to analyze the characteristics of bolted connections, experimental work must be performed. In this thesis, two groups of test sets were conducted: the first group consisted of six specimens with 1 inch (25.4mm) rod thickness and the other 1.5 inch (38.1mm) rod thickness. The purposes of the experimental work are:

- To estimate matters related to bolt force
- To estimate separation of the flanges

Measurement of bolt force is not easily performed since the bolts are placed in the flanges without any gap between bolt head (or nut) and flanges: It is impossible to attach strain gages on the bolt directly. Instead of direct measurement, an alternative method using a *load cell* was devised. According to the force equilibrium method, force applied to the bolt was converted; detailed description is given later in this chapter.

Estimation of the gap of the two flanges following flange-separation was measured directly by a digital caliper.

The specimens showed typical characteristics such as passing the elastic range, showing yielding and necking, and finally failure, in that order (refer to Fig. 2.2).

3.1.1 Detailed dimensions of the specimens

Twelve pairs of flanges, twenty four pieces of bolts, and two pieces of load cells were prepared to conduct this experimental work. First, detailed dimensions of the flange, the bolt, and the load cell are listed in Fig.3.1 to 3.3, and Table 3.1 to 3.3, respectively.

For convenience of the finite element modeling, some dimensions were slightly modified (e.g. threaded part of the bolt and the rod).

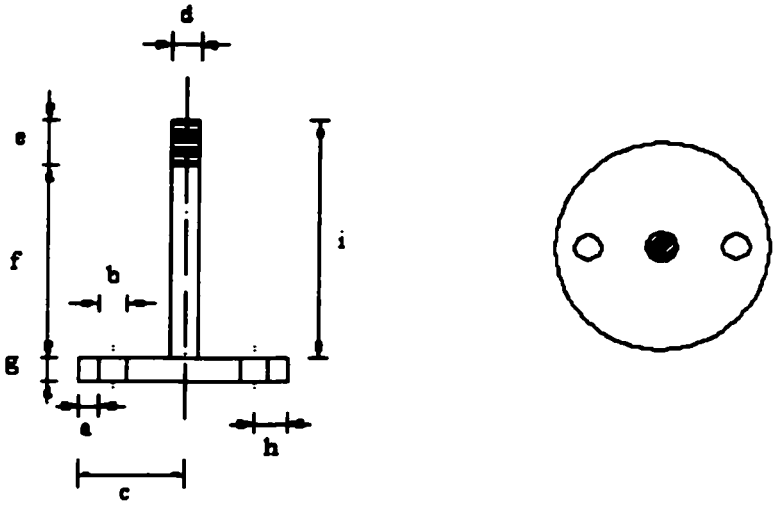

Fig.3.1 Detailed dimensions of the flange

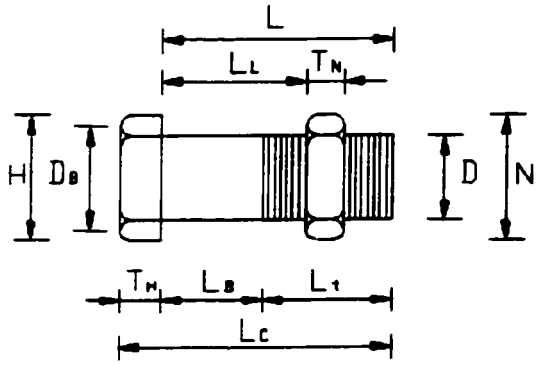

Fig.3.2 Detailed dimensions of the bolt (A325, 5/8 inch)

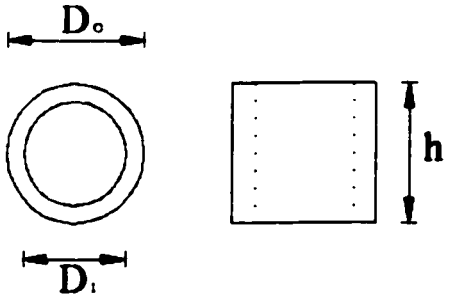

Fig.3.3 Detailed dimensions of the load cell

Table 3.1 Dimensions of the flange

	(a)	(b)	(c)	(d)	(e)	(f)	(g)	(h)	(i)
GROUP 1									
S1	17.28	17.65	88.57	25.64	44.04	156.16	20.03	28.64	200.20
S2	17.67	17.52	88.50	25.53	43.34	177.73	19.53	29.27	221.07
S3	17.58	17.37	88.19	25.70	45.71	173.86	19.92	29.08	219.57
S4	17.22	17.80	88.67	25.86	45.07	170.36	19.83	29.01	215.43
S5	18.18	17.99	88.79	25.70	44.88	178.18	19.78	29.76	223.06
S6	18.35	17.76	88.38	25.78	46.33	176.00	19.89	30.11	222.33
USE	17.00	18.00	89.00	26.00	44.00	172.00	19.00	29.00	216.00
Drawing	-	-	88.90	-	38.10	165.10	19.05	-	203.20
GROUP 2									
F1	20.49	15.37	88.84	38.27	52.14	252.38	19.56	28.17	304.52
F2	20.67	16.13	88.14	38.26	52.44	245.61	20.81	28.73	298.05
F3	19.79	16.86	88.58	38.34	52.88	250.71	20.34	28.22	303.59
F4	19.73	17.00	88.55	38.25	52.42	247.48	19.80	28.23	299.90
F5	19.85	16.86	88.59	38.19	52.81	251.33	20.27	28.28	304.14
F6	20.34	16.26	88.44	38.53	52.59	246.70	20.17	28.47	299.29

Unit: mm
Detailed measurement is in Appendix A.
USE for F.E.A

Table3.2 Dimensions of the bolt

	L	L_L	T_N	T_H	L_B	L_t	L_C	D	D_B	H	N
Dim.	95.25	63.00	15.36	12.18	50.80	44.45	107.43	15.875	22.35	23.58	26.61
USE	-	63.00	13.00	13.00	-	-	-	16.00	-	24.00	24.00

Unit: mm
Bolt: A325, 5/8"
USE for F.E.A

Table3.3 Dimensions of the load cell

	Load Cell A	Load Cell B	Ave.	USE
D_o	35.95	35.92	35.94	36.00
Di	17.34	17.11	17.22	17.00
H	24.89	24.87	24.88	25.00

Unit: mm
USE for F.E.A

3.1.2 Material properties of the specimens

Flange material (ASTM A572-50-TYPE2-00) tested by Gerdau Courtice Steel Inc., Cambridge, ON, Canada shows that yielding strength – 54,548 psi (376 MPa), 57,143 psi (394 MPa) and tensile strength – 77,656 psi (535 MPa) and 81,403 psi (561 MPa). To find Young's modulus, the average value of the yielding strength: 385MPa and 0.2% offset method were used.

- Yield strength (σ_y): 55,845 psi (385 MPa)
- Tensile strength (σ_u): 79,529 psi (548 MPa)
- Young's Modulus (E): 27,922 ksi (192.5 GPa)

According to ASTM, bolt (A325, 5/8") material properties are

- Yield strength (σ_y): 92,000 psi (635 MPa)
- Tensile strength (σ_u): 120,000 psi (825 MPa)
- Young's Modulus (E): 46,000 ksi (317.5 GPa)

Properties of the load cell (AISI-4140) are

- Yield strength (σ_y): 62,000 psi (427 MPa)
- Tensile strength (σ_u): 89,000 psi (613 MPa)
- Young's Modulus (E): 31,000 ksi (213 GPa)

3.2 Experimental Set-Up

3.2.1 Strain gages

Electric strain gages made by Kyowa Electronic Instrument Co. Ltd., Tokyo, Japan were used to measure strain of the load cell. Physical properties and detailed description are shown in Table 3.4. Before attaching strain gages, the surface of the load cell was polished and cleaned using Isopropyl Alcohol, M-Prep Conditioner A, and M-Prep Neutralizer 5A, in order. After polishing, the strain gage was attached with transparent tape not to be moved during attaching. M-bond 200 catalyst was applied on

the bonding surface of the gage and then, glue was applied so that the gage and load cell would not be separated. Finally, wires were connected with gages and coating material was put on the load cell (Fig.3.4).

Table 3.4 Properties of the strain gage

Type	KFG-5-120-C1-11
Temperature Compensation For	Steel
Gage Length	5 mm
Gage Factor (24°C, 50%RH)	2.11±1.0 %
Adoptable Thermal Expansion	11.7 PPM/°C
Transverse Sensitivity	0.40 %
Applicable Gage Cement	CC-33A, PC-6

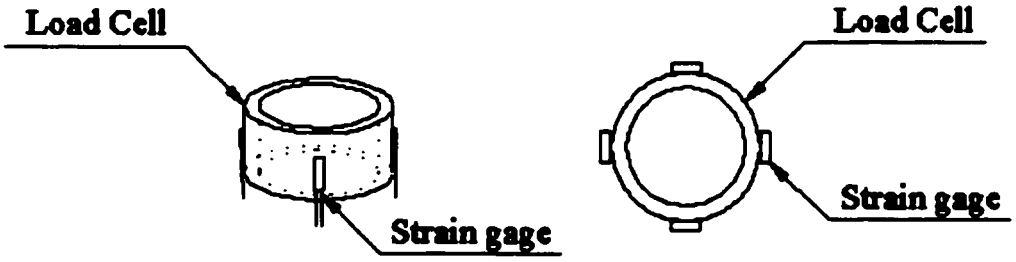

Fig. 3.4 Strain gage set-up

3.2.2 Set-up for measuring elongation of the bolts

After preparing the strain gages, the load cell was assembled within a bolt set: bolt and nut. Wires from the four strain gages were connected to the Data-Scan System – strain indicator using the quarter bridge method (refer to Fig.3.5 and Appendix G. Photo 3).

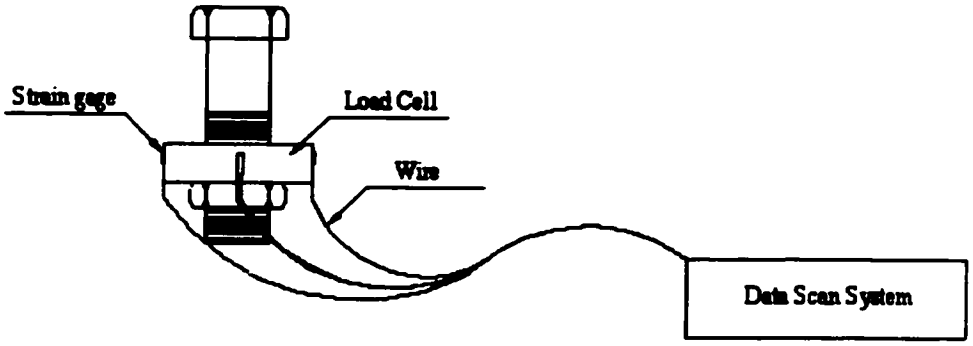

Fig.3.5 Data Scan System (flanges omitted)

3.3 Experimental Procedure

The assembled specimen was placed on the Universal Testing Machine (refer to Fig.3.6) made by Tinus Olsen. The external load was applied until the specimen failed. As expected, the failure load was close to the value theoretically calculated. As the external load was applied, separation of the flanges and strain of the load cell were measured by a digital caliper and strain indicator, respectively.

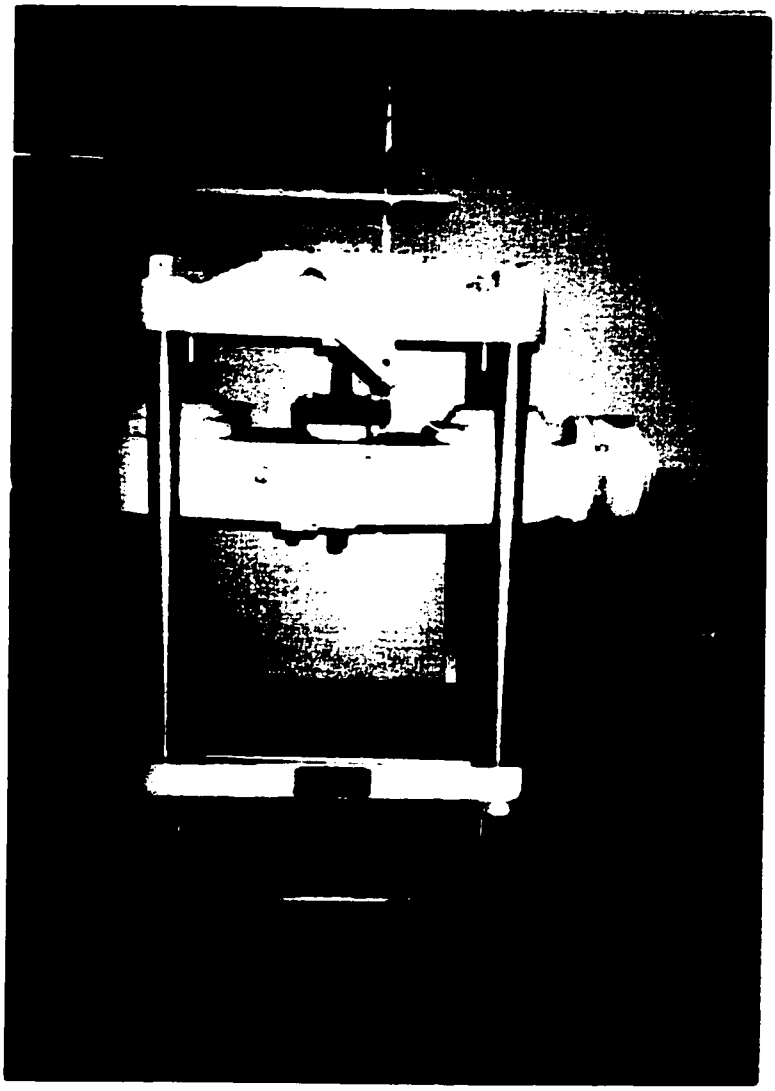

Fig.3.6 Universal Testing Machine

3.4 Determination of Bolt Force

3.4.1 Determination of the preload of the bolt

In order to determine preload of the bolts, an indirect method was used as drawn below

$$F_{pr} = \Psi * B_{min} \qquad (3\text{-}1)$$

where,

F_{pr} = Preload of the bolt (kN)

Ψ = Load factor

B_{min} = Minimum bolt force (kN) suggested by CISC

According to the experimental results conducted by Corro (1998), Ψ = 1.496 is obtained (bolt: 3/4" and 1/3 turn of nut) [5]. Considering the difference in the bolt size and the degree of turning the nut, Ψ was assumed to be 1.3 and this value was verified with the tedious *trial and error method*. To confirm this factor, furthermore, the results were compared with the experimental data conducted by Sherbourne and Bahaari (1996) [11]. They agreed very well with each other.

3.4.2 Application of strain data

In order to estimate bolt force, a load cell was used; yet strain data from the experiment had to be checked before use because both sides of the load cell face different areas, flange and nut (refer to Fig.3.7). That is, strain gages located on the middle of the load cell can represent just part of the strain used for calculating force since the forced areas are different.

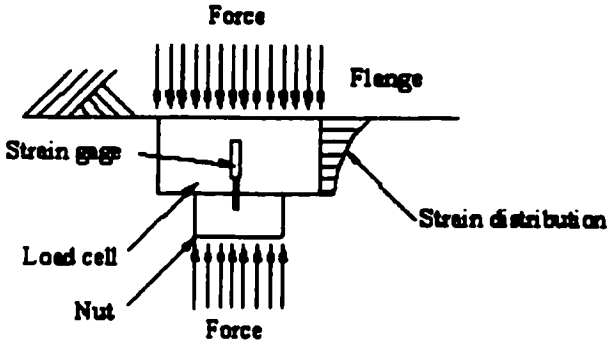

Fig.3.7 Strain distribution on the load cell

To overcome this unequal strain problem, the finite element method was used to verify whether the strain values obtained from the experiment can be used or not. The basic concept of this method is to figure out the relation between strain on the middle and strain on the end sides toward the nut and the flange. The reason is shown in Fig.3.7; see the strain distribution. Without any flange and bolt, just a load cell was modeled and distributed loads, 135 kN equivalent, were applied on both sides as in Fig. 3.7. According to this method, the following strains were found: the top-strain was $964*10^{-6}$; the mid-strain was $478*10^{-6}$; and $130*10^{-6}$ was calculated for the bottom-strain (refer to Fig.3.8 and Appendix D). Therefore, the average strain was $524*10^{-6}$. Thus, using the mid-strain sounds to be a reasonable strategy. Therefore, strain gages on the current location can be used as average strain values through the whole load cell without severe trouble.

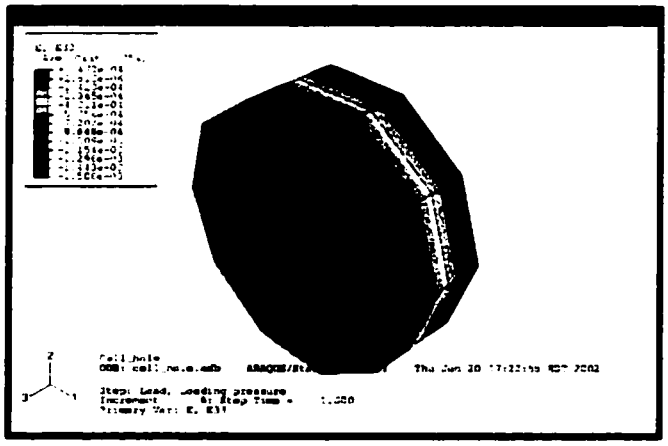

Fig.3.8 Strain distribution checking in the load cell

3.4.3 Calculation of the bolt force

Basically, knowing the bolt force directly seems impossible so the applied force on the load cell is assumed to be equal to the force in the bolt according to equilibrium condition (refer to Fig.3.7). Hooke's law was used to estimate the force in the fastener and, of course, during loading, the load cell was in the elastic range (yielding starts from 333 kN in this case, refer to *3.1.2 material properties of the specimens*).

$$F = E \varepsilon A \qquad (3\text{-}2)$$

where,

F = Bolt force

E = Young's modulus of the load cell

ε = Axial strain

A = Cross-section area of the load cell

Table 3.4 Increase of bolt force (S-1)

T	0	15	30	45	60	75	90	105	120	135	143
ε (ave.)	0	4.62	10.80	18.80	61.10	179.00	278.00	382.00	499.00	626.00	Fail
ΔB	0	0.29	0.69	1.21	5.88	11.56	17.94	24.64	32.18	40.36	Fail

*T=external load/bolt(kN), ε(ave.) = average strain (10^{-6}) from experiment, ΔB (increase of bolt force (kN) by Eq.4-2
Preload = 110 kN (minimum value = 85 kN)
Failure load =average failure load of group2
Detail data shown in Appendix C

As mentioned, rod failure was observed before bolt failure in group 1, so in order to complement the data, the average failure load of group 2 was used in Fig. 3.9 and Table 3.4. And, to compare the round bar connection with the T-stub connection, experimental data obtained from Sherbourne and Bahaari (1996), S.&B., were indicated in Fig.3.9. Even though the latter was performed with a T-stub with a thickness of 20mm, it was 1mm bigger than the specimen used in this study, other geometric conditions are also within reasonable accuracy, nevertheless the results agreed very well.

Here, one interesting phenomenon was reported (Struik and Back, 1969). It is that pre-tensioning of a bolt does not affect the bolt-failure-load. To put it simply, whether the preload is high or low, the bolt still fails at almost the same load.

From an observation of Fig. 3.9, bolt failure was affected by a slight eccentricity in the case of the round bar connection and this eccentricity effect was almost negligible in the T-stub connection (It is presumably due to location of the bolt). According to hand

calculation, the bolt is supposed to fail at 163 kN and it failed when the applied load was 143 kN for the round bar connection and 160 kN for the T-stub case, respectively.

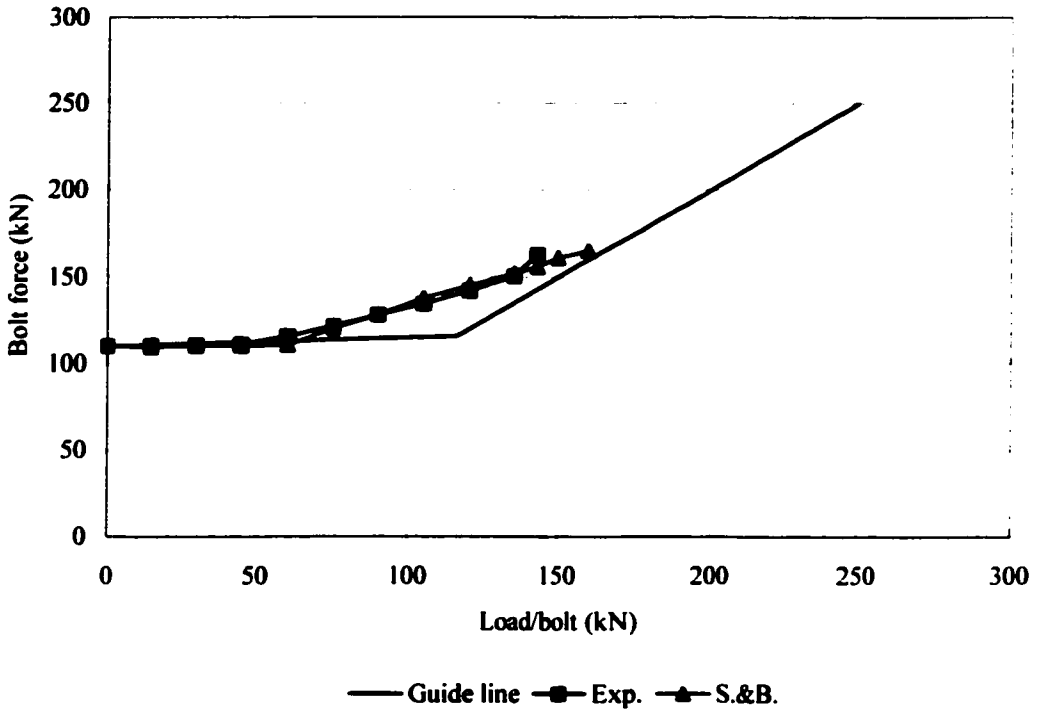

Fig 3.9 Bolt force obtained from the experiment (S-1)

3.5 Relation between Prying Action and the External Load

Prying action is a peculiar characteristic under tensile loading. Bolt force seems to be the same with the applied load but, due to this action, additional force must be considered. This prying force is dependent upon stiffness and thickness of the gripped material . That is, if the material is very stiff or very thick, prying force becomes minimized, even of zero value. The problem, however, is that material which is too stiff or thick can induce uneconomical or over-estimated design. Therefore, figuring out the appropriate prying force can serve as a guide to the best design.

Table 3.5 Prying force

T	0	15	30	45	60	75	90	105	120	135
B	110.00	110.29	110.69	111.21	115.88	121.56	127.94	134.64	142.18	150.36
G	110.00	110.75	111.50	112.25	113.00	113.75	114.50	115.25	120.00	135.00
P	0	0	0	0	2.88	7.82	13.44	19.40	22.19	15.37

T: External load/bolt, B: Bolt force, G: Guide line, P: Prying force, unit:kN

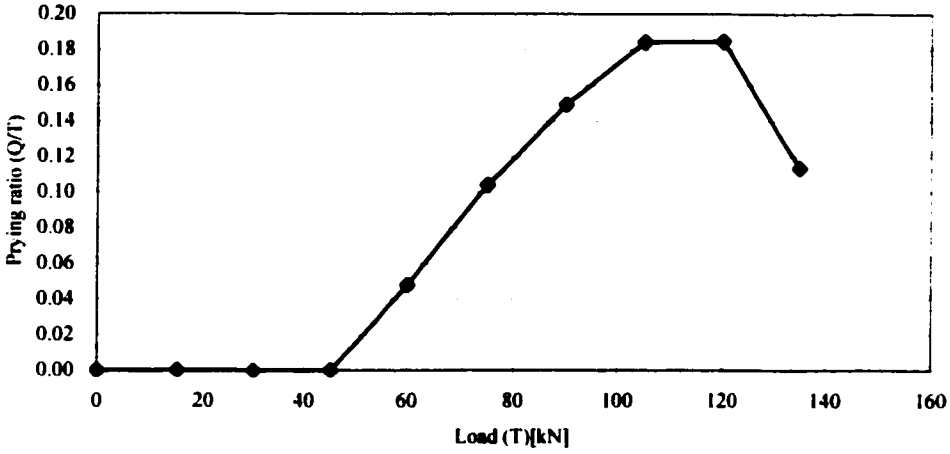

Fig.3.10 Prying ratio

Negative values were observed during the experiment in prying force up to the 45 kN tensile load; so it was regarded as zero and the maximum ratio was observed as 18% of the external load (theoretically, the prying ratio is possible up to 33%; CISC). This means that peak prying force occurs at load level around 105 to 120 kN. Prying force is not desirable because it increases stress in the bolt. Hence, when it comes to designing bolted connections, thickness of the flanges should be found to make prying force as small as possible.

3.6 Applicability of T-Stub Equations to Round Bar Connection

T-stub equivalent equations were popular, in general, and are mentioned and explained in Chapter II. Further detailed calculations appear in Appendix B (CISC or *Canadian Institute of Steel Construction* and VDI or *Verein Deutscher Ingenieure - German Engineering Society* handbook, respectively, and more detailed descriptions are referred to each book)

$$B = \left[1 + \frac{\delta\alpha}{(1+\delta\alpha)}\frac{b}{a}\right]T \qquad (2\text{-}1)$$

$$F_B = (1 + s)\,F_{pa} - \Delta F_m - \Delta F_{EI} + \Phi_{en} L_X \pm \Phi_{en} K_J''(\Delta L_J - \Delta L_B) \qquad (2\text{-}2)$$

However, no equation was developed for the solid round bar connection. In this chapter, applicability of T-stub equivalent equations was reviewed.

Table 3.6 Bolt force calculated using T-stub equations

T	0	15	30	45	60	75	90	105	120	135
Exp.*	110.00	110.39	110.69	111.21	115.88	121.56	127.94	134.64	142.18	150.36
Eq.2-1	-	-	-	-	-	-	131.69	161.69	-	-
Eq.2-2	110.00	119.70	127.20	134.70	142.20	149.70	157.20	164.70	-	-

*Exp.: bolt force from experiment , unit:kN

At a load of 105 kN, an error is shown to be 16.7% and 18.3% for Eq.2.1 and Eq.2.2, respectively, with the experimental value. At this load level, the prying ratio was recorded to be the highest (refer to Fig.3.10). The bolt fails at around 163 kN; so Eq.2-1 and Eq.2-2 cannot be applied after a load level of 120 kN. And Eq.2.4 shows linear behavior from 0 to 105 kN, so only two values were shown since values below 90 kN were useless. T-stub experimental data (Sherbourne and Bahaari, 1996), S.& B., also agreed very well. According to Fig.3.11, maximum prying force occurred around the external load at 105 kN. Therefore, applicability of Eq.2.1 and Eq.2.2 shown above sounds very reasonable.

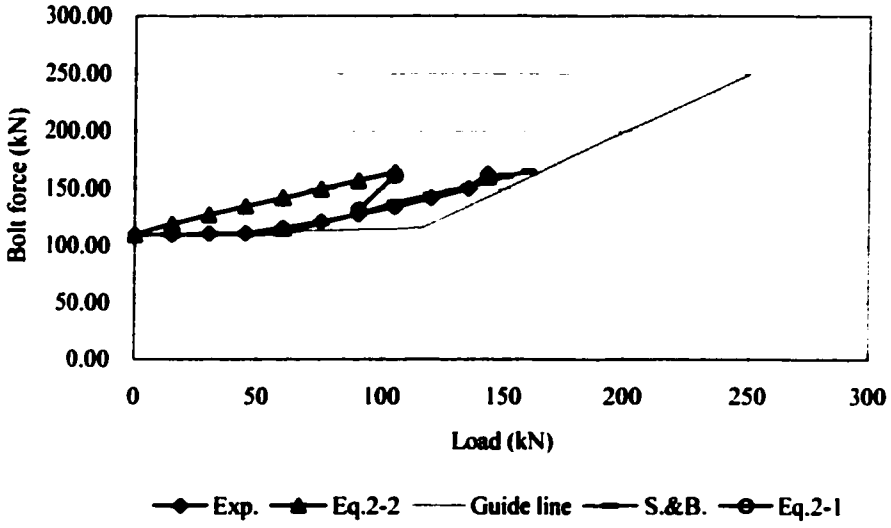

Fig.3.11 Application of T-stub equivalent equations

Usually, connections are designed within a range in which the flange does not separate. The AISC recommends σ_{all} should be 303 MPa for A325 bolt (or 60 kN/bolt for 5/8 inch). Therefore, all values in Fig.3.11 are shown in the very safe range, and the value recommended almost does not exceed the preload of the bolt. Hence, design criteria stays in the very safe range in any case. In addition, considering conservative design of the flange connection, the T-stub equivalent equations can be applied for solid round bar connections.

3.7 Gap Development of the Flanges under the External Tensile Load

For measuring the gap between flanges, eight locations or two direction diagonal for group 1 and four locations or one diagonal for group 2 (Fig.3.12) on the flange were measured using a digital caliper directly. In group1, from specimen 1 (S-1) to specimen 6 (S-6), except for the specimen 2 (S-2), with preload and the specimen 2 (S-2) without preload, finger tight, were used and the preload was applied to every specimen from F1 to F6 for group 2. The rods failed first, as expected, before the bolts failed in all specimens (threads failed in specimen 6 (S-6)) in group1. However, bolt failures were witnessed in group2.

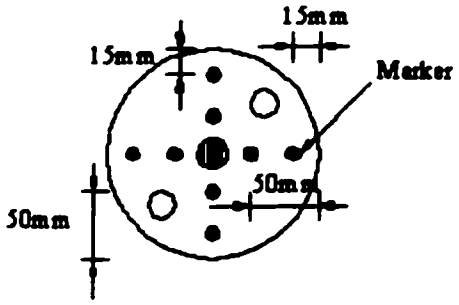

Fig.3.12 Marking for measuring flange-separation

During the experiment, several slipping-phenomena were witnessed in group1. A summary of the results is shown in Table 3.7. As shown in Table 3.7, deformed shapes of the flanges show asymmetry at failure. It may be induced due to imperfection of the specimens. By witnessing that bolt failure occurred on only one out of the two bolts, imperfection and asymmetry are proved reasonably. Typical gap-development, corresponding to the external load, of the flanges is shown in Fig.3.13.

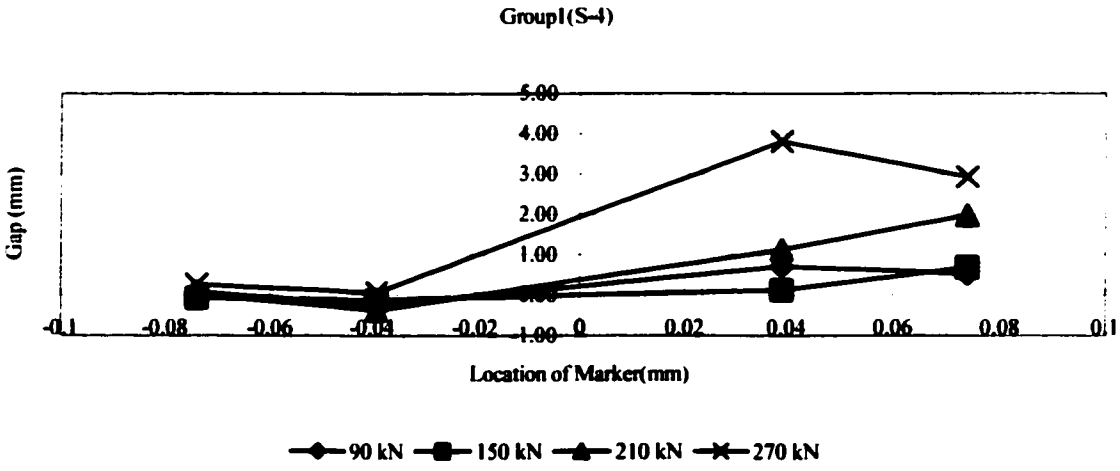

Fig 3.13 Typical gap-development of the flange (S-4)

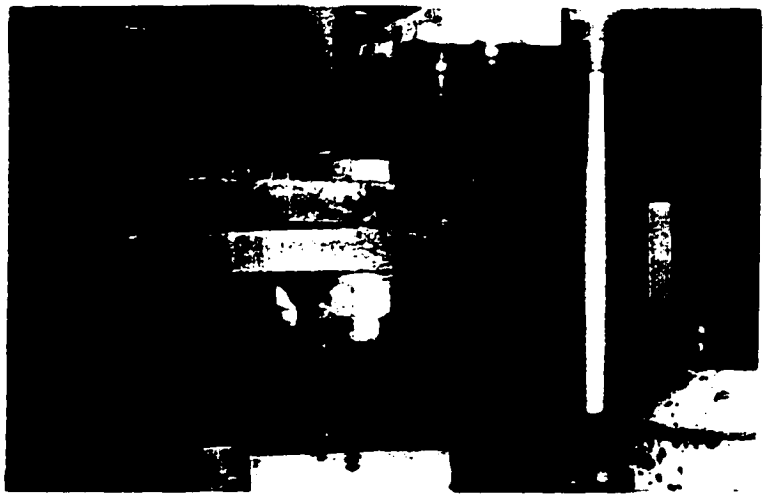

Fig 3.14 Asymmetric deformed shape of flanges (S-4)

Table 3.7 Summary of test data

	Preload	Load cell	Failure load (kN)*	Deformed shape	Remark
			GROUP1		
S1	Yes	Yes	276	Asymmetric	
S2	No	No	274	Asymmetric	
S3	Yes	No	281	Asymmetric	
S4	Yes	No	282	Asymmetric	
S5	Yes	No	274	Asymmetric	
S6	Yes	No	230	Asymmetric	Thread failed
			GROUP2		
F1	Yes	No	288	Asymmetric	
F2	Yes	No	284	Asymmetric	
F3	Yes	No	293	Asymmetric	
F4	Yes	No	286	Asymmetric	
F5	Yes	No	282	asymmetric	
F6	Yes	No	287	asymmetric	

*Failure load = rod failure load for group1 and bolt failure load for group2, total applied load
Detail data shown in Appendix C

CHAPTER IV

ANALYTICAL MODELING

4.1 General

In the early of 1900's, researchers suggested a new methodology to analyze stress. This method was called *Lattice analogy* and has been developed for years. In the 1940's, mathematicians developed a new concept, based on the extension of the former theory, called *Finite Element Method.* With the unbelievable development of computer industry, this new method was also developed with great speed. Nowadays, dependency on the finite element analysis (FEA) has become essential in every engineering field.

The basic concept of the FEA is dependent upon *discretization* to depict the real structure. The classical methods solve the given problems exactly with the differential equations. FEA, instead, approaches the results using discretization called *modeling*. This method solves problems approximately, not accurately. Meanwhile, the results of analyses are quite reliable at reasonable cost in almost every engineering field. That is the reason FEA is so popular.

General formulations for the FEA are performed on the basis of the stiffness matrix and it is defined as the ratio of force to displacement. Therefore, it can be written as

$$\{P\} = [K]\ \{D\}$$

where, {P} : Applied load vector

[K]: Structural stiffness matrix

{D}: Displacement vector

4.2 Analytical Modeling

4.2.1 Geometry and material properties

As explained in Chapter I, three dimensional numerical models were developed. For convenience, two dimensional models, sometimes, are analyzed using a reduction factor recommended in ASME Section VIII Div2 (refer to ABAQUS example manual 4.1.3-3). However, as this is an approximate modeling technique, there is a need to develop three dimensional models in this thesis to perform more accurate analyses. The geometry and dimensions are slightly modified to simplify the modeling (refer to Chapter III). The model consists of upper and lower flanges, a bolt, and a load cell. Some parts are not included in this modeling such as welding, and the threaded part of the rod and the bolt.

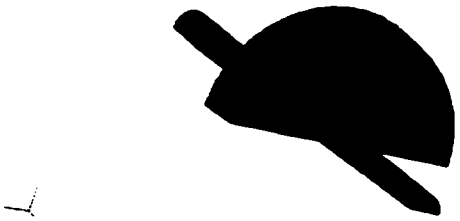

Fig. 4.1 Developed 3D numerical models

Material properties were given to the model such as elastic and plastic cases. The elastic property gave short running times. Elastic and plastic properties cannot be compared with each other since the categories are quite different. The elastic model was not mentioned here because this thesis concerns range above the elastic limit. When it comes to just design, elastic property brings reasonable results. There is some deficiency since a material property test was not conducted. Material test data reported by Back and Zoetemeijer (1972) were quoted to supplement the deficiency. The test data showed that σ_u reaches when strain reaches 21times yielding strain, 21 ε_y, for flange material and 8 ε_y for bolt material.

4.2.2 Surface interaction

Basically, this problem is in the category of contact analysis. It means, severe discontinuity iterations are supposed to be calculated. Surface interactions were defined in several parts as indicated below:

(1) Between the underside of the bolt and upper flange
(2) Between underside of both upper and lower flanges
(3) Between contact surface of the load cell and lower flange
(4) Between contact surface of the load cell and underside of the bolt

In particular, (1), (3), and (4) were constrained using the TIE parameter since once they are attached, they are not separated. The friction coefficient of 0.3 was given to (2).

4.2.3 Loading and boundary conditions

To make matters simple, only half of the whole flange was modeled owing to its symmetric condition. One point in the upper flange was fixed to prevent numerical singularity. Two steps were defined in the whole analysis. First, a clamping force or *preload* was given to the bolt. The pretension section was specified around one quarter of the bolt shank (refer to Fig.4.2). Second, the distributed load was defined on the end-surfaces of the both rods.

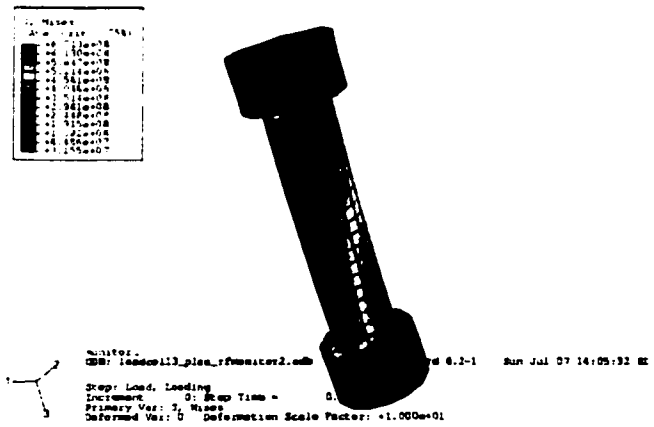

Fig 4.2 Pre-tensioning of the bolt

4.2.4 Results and discussion

All analyses were performed as small-displacement analyses. As expected, the circumference of the bolt-hole was stressed after the preloading step. As the external loads are applied, the flange started to separate and stress distribution was expanded toward the edge of the flanges. The results obtained from the finite element analysis showed similarity with the theoretical calculation. Yet, a slight difference was observed against the experimental data (refer to Fig. 4.4). The reason can be explained below:

1) Exact material test was not conducted.
2) Bolt was modeled without threaded part (i.e., there is a slight difference between the nominal and stress areas)
3) Preload was calculated relying on the literature.
4) Geometrical imperfection was not considered in the simulations.

As was shown in Chapter III (refer to 3.5), the external load level 105 kN was observed as a critical range in the numerical analysis too. During the experiment, asymmetric deformed shapes were observed but symmetric deformed shapes were found in the FEA.

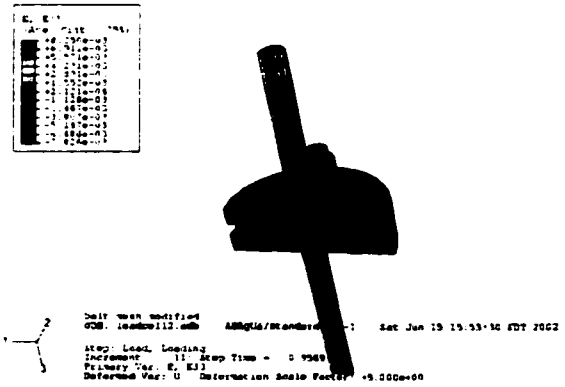

Fig.4.3 Symmetric deformed shape

The purpose of analytical modeling is to improve general understanding regarding bolted flange connections. By performing the finite element analysis, the phenomena

related to the connection were revealed clearly from its behavior, indicating how to deal with this kind of problem.

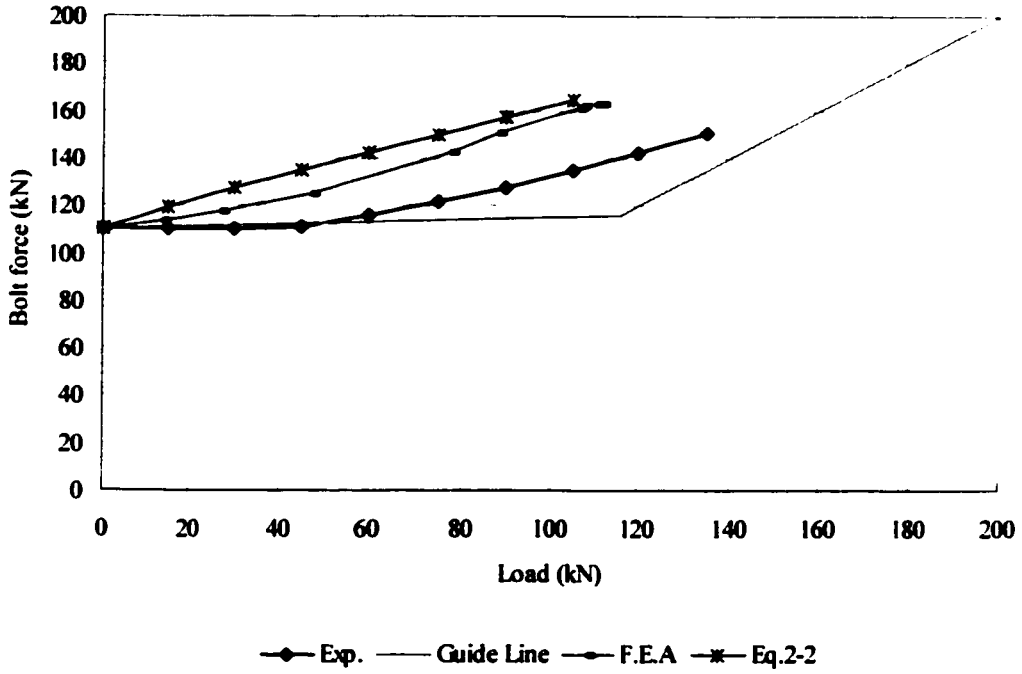

Fig. 4.4 Comprehensive comparison among theory, experiment, and F.E.A.

CHAPTER V

DESIGN RECOMMENDATIONS

5.1 General

Salmon and Johnson defined structural design as a mixture of art and science [15]. Design was performed by relying too heavily on engineers' experience and intuition before computer age. But design and analysis methods of the current industry are greatly improved by following the development of a digital computer. Even though the dependency becomes bigger and bigger, engineers' experience must still be one of the most important and valuable factors in design. In addition to this, if a systematic design method is suggested, it couldn't be better. As mentioned in Chapter I, proposing a systematic design method for solid round bar connections is one of the purposes of this thesis and it goes without saying that the proposed method guides engineers to an easy design approach when it comes to a round bar connection under tensile loading, step by step.

There can be two design methods such as Allowable Stress Design Method and Limit States Design Method, and they are also called Working Stress Design Method and Plastic Design Method, respectively. The concept of the first method is that any value used is the critical value divided by a factor of safety and it is represented as

$$Allowable = \frac{Critical}{F.S.}\left(or\ \frac{Yielding}{F.S}\right) \qquad (5\text{-}1)$$

As was shown in Eq.5-1, this design method deals with only elastic range. Hence, it is a safer design method and many Asian countries like South Korea accepted this method when it comes to steel design. However, considering effective-cost-design, this must be higher than the Limit States Design Method since the range is narrower.

The concept of the Limit States Design Method is considering plastic limit or the ultimate point, over the critical limit. This method is more effective but a designer must be very aware of material behavior or collapse mechanism because, after the critical point, permanent deformation occurs.

Effect of Reduction Factor x *Strength* ≥ *Effect of Load Factor* x *Load* (5-2)

Nowadays, a relatively new method is employed called LRFD or *Load and Resistance Factor Design*. This method also considers and expands the design area up to plastic range and this one is a very cost-effective design approach, but is more complicated than the other two methods mentioned above.

$$\phi R_n \geq \gamma_n \Sigma \gamma_i Q_i \qquad (5\text{-}3)$$

where,

i = Load like DL, LL,W,S, etc.

R_n = Nominal strength

Φ = Load and resistance factor (e.g. 0.75 for bolt fracture)

γ_i = Overload factors

Q_i = Product of load effect.

5.2 Allowable Stress Design

The basic definition of stress can be expressed

$$B_u = A_s \sigma_u \qquad (5\text{-}4)$$

where,

B_u = Maximum tensile load of bolt

A_s = Stress area

σ_u = minimum specified tensile strength (e.g. 90 ksi or 620 MPa for A325)

Converting the stress area, A_s, to nominal bolt area, A_b, and using a factor of safety .

$$B_{all} = \frac{(\alpha A_b)\sigma_u}{F.S.} \qquad (5\text{-}5)$$

And Kulak et al. (1987) suggested F.S. = 2.0, α = 0.75, so

$$B_{all} = 0.375 A_b \sigma_u \qquad (5\text{-}6)$$

By considering general bolt-flange connection behavior, Eq.5-6 can be expressed

$$B_{all} \geq T + Q \qquad (5\text{-}7)$$

5.3 Limit States Design

This method in bolt design is very similar with Allowable Stress Design. A load reduction factor, Φ, is required instead of a factor of safety and Kulak et al. (1987) suggested that Φ=0.85 and γ=1.7 agreed well with past experience [7].

$$\phi B_{used} = \gamma(\alpha A_b)\sigma_u \qquad (5\text{-}8)$$

5.4 Determining Length of Flange Tributary to Each Bolt

Usually the length of the flange tributary of each bolt or *bolt pitch* denotes distance between bolts or the area that the bolt can cover in connection. As shown below, determination of bolt pitch is easy in T-stub by dividing the length between two bolts. However, in a round bar connection, it is not that easy, owing to its geometry.

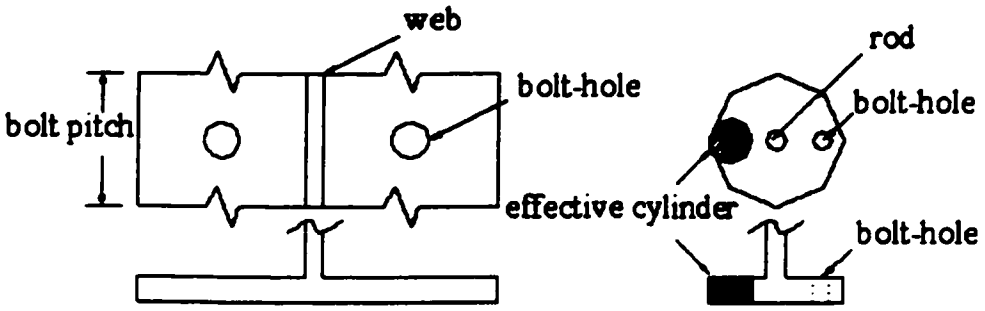

(a) T-stub (b) circular flange

Fig.5.1 Comparison of bolt pitch

Hence, the effective cylinder is suggested in this thesis for a round shape flange. The maximum distance from the center of the bolt-hole to the tip of the flange can be considered as the radius of the effective cylinder. It also means that the bolt force affects in the range of the cylinder like the bolt-pitch of the T-stub. So, when Eq.2-1 and Eq.2-2 are used for solid round bars and round shape flanges, the pitch is suggested.

5.5 Proposed Design Steps

5.5.1 General

In this chapter, systematic design steps will be proposed in order to help engineers to design. A sample design for solid round bar connections is shown in Appendix E.

When it comes to solid round bar connections, the bar must be thick enough not to fail by the external load before the bolts fail.

$$d \geq \sqrt{\frac{4T}{\sigma_y \pi}} \qquad (5\text{-}9)$$

where,

d = Diameter of the rod

T = External load

σ_y = yielding stress

Usually circular flanges are recommended to avoid stress concentration and to distribute stress equally. The bolt-hole in the flange is generally bigger than the bolt diameter by 2 mm or so, and distance from the tip of the flange to the center of the bolt-hole does not exceed 1.25 times of the distance from the bar to the center of the hole. When it comes to *length of flange tributary to each bolt*, the value is recommended in general to be 4 to 5 times of bolt diameter ($4d \leq p \leq 5d$). Referring to specification, service load is determined considering various loads like Dead Load, Live Load, Wind, Ice, etc.

After service load is determined, the number and type of bolts are selected. Referring to *Structural fastener* section in Chapter II, either A325 or A490 can be selected. According to the analysis of round bar connections in Chapter III, the T-stub design equations can be employed to round bar connections without significant trouble. Therefore, Eq.2-1 and Eq.2-2 are recommended, recalling that these are conservative in round bar

connections. Bolt force used in design, B_{used}, must exceed a certain level of force whether Allowable Stress Design or Limit States Design used and one more, of course, the sum of each bolt force must be greater than the service load. To avoid complicated calculation. Table 3.13 and Figure 3.2 in the Handbook of Steel Construction by CISC [2] can be used for convenience, when exact data are not required.

Calculation of flange thickness is related closely to location of the bolt-holes. Like other general design steps, basic geometry is determined for designing briefly including the location of the bolt-hole, first. Eq.5-10 was slightly modified from the Handbook of Steel Construction by CISC and suggested to determine the thickness. Detailed notations are omitted to avoid redundancy.

$$\sqrt{\frac{KP_f}{(1+\delta)}} \leq t \leq \sqrt{KP_f} \qquad (5\text{-}10)$$

where,

$K = 4\ b'\ 10^3 / (\Phi\ p\ F_y)$

$\delta = 1\text{-}d'/p$

* detailed notations are referred to Chapter III

After knowing the possible range of the thickness, engineering decision is required to identify the required thickness.

At this point, almost every thing is known about bolted connections for a solid round bar from bolt resistance to flange geometry. Before revealing the design model, several things must be checked.

1) Connection capacity

$$C = (t^2/K)(1+\delta\alpha)\, n \geq \text{Total load applied} \qquad (5\text{-}11)$$

where,

t = thickness of the flange (mm)

n = number of the bolt

$$\alpha = \left(\frac{KT_r}{t^2} - 1\right) \times \frac{a'}{\delta(a'+b')} \quad , 0 \leq \alpha \leq 1.0$$

$K = 4\, b'\, 10^3 / (\Phi\, p\, F_y)$

$\delta = 1 - d'/p$ (mm)

$T_r = \Phi_\beta\, 0.75\, A_b \sigma_u$

* detailed notations are referred to Chapter III

2) Bolt force capacity

$$B = \left[1 + \frac{\delta\alpha}{(1+\delta\alpha)} \frac{b}{a}\right] T \qquad (2\text{-}1)$$

$$F_B = (1+s)\, F_{pa} - \Delta F_m - \Delta F_{EI} + \Phi_{en} L_X \pm \Phi_{en} K_J''(\Delta L_J - \Delta L_B) \qquad (2\text{-}2)$$

Bolt force calculated by Eq.2-1 or Eq.2-2 must be exceeded by both the applied external load and tensile resistance of bolts or T_r must be greater than the bolt force.

$$\sum_{i=1}^{n} B_i \geq \sum T \text{ and } T_r \geq B \qquad (5\text{-}12)$$

where,

B = Bolt force

n = Number of bolts

T = Applied external load

T_r = Factored tensile resistance of bolts, Φ_β 0.75 $A_b\sigma_u$

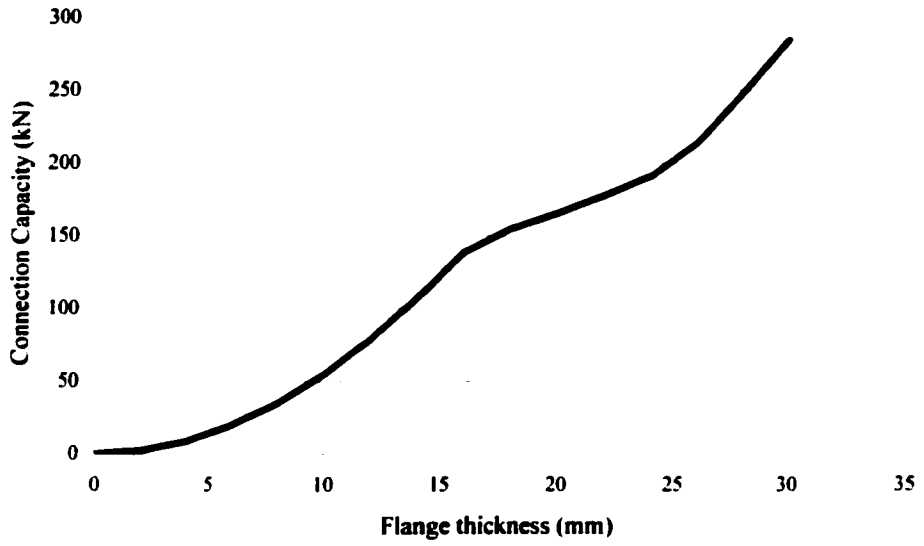

Fig.5.2 Connection capacity

Fig.5.2 shows a typical example of connection capacity of a bolted round bar connection using Eq.5-11. This graph induces connection capacity corresponding to flange thickness. Once achieving this graph, a designer can easily choose maximum external load and flange thickness. Next, the step-by-step design method will be presented and though it seems somewhat redundant, it is necessary to show every step for its continuity and self-standing-guide.

5.5.2 Step-by-step design

Step1: Determine basic geometry.

1-1) Rod diameter = $d \geq \sqrt{\frac{4T}{\sigma_y \pi}}$

1-2) Assume bolt size and property (e.g. M22 and A325)

1-3) Hole diameter = nominal bolt diameter + 2 mm

1-4) Bolt pitch = 4d ≤p≤ 5d and assume this value as $2a$

1-5) Distance from the center of bolt hole to the tip (a) of a flange and the rod (b).

here $b \geq a / 1.25$

1-6) Radius of a flange = a + b + d / 2

Step2: Determine thickness of a flange.

2-1) $K = 4\, b'\, 10^3 / (\Phi\, p\, F_y)$

where,

b' = b - d/2 (mm)

Φ=0.9

F_y = yield strength (MPa)

p = bolt pitch

2-2) δ = 1 - d'/p (mm)

where,

d' = hole diameter (mm)

2-3) $\sqrt{\frac{KP_f}{(1+\delta)}} \leq t \leq \sqrt{KP_f}$

where,

P_f = external load / bolt

2-4) Determine t

Step3: Design check.

3-1) $\alpha = \left(\frac{KT_r}{t^2} - 1\right) \times \frac{a'}{\delta(a'+b')}$ $, 0 \leq \alpha \leq 1.0$

where,

$a' = a + d / 2$ (mm)

$b' = b - d / 2$ (mm)

$K = 4\, b'\, 10^3 / (\Phi\, p\, F_y)$

$T_r = \Phi_\beta\, 0.75\, A_b \sigma_u$

3-2) $C = (t^2 / K)\,(1+\delta\alpha)\, n \geq$ Total load applied

3-3) $\alpha = \left(\frac{KP_{fr}}{t^2} - 1\right) \times \frac{1}{\delta}$ for 3-4)

3-4) $B = \left[1 + \frac{\delta\alpha}{(1+\delta\alpha)} \frac{b}{a}\right] T$

3-4) $\sum_{i=1}^{n} B_i \geq \sum T$ and $T_r \geq B$ (if OK, then STOP : if not, REPEAT)

CHAPTER VI

DEVELOPMENT OF DESIGN PROGRAM

6.1 General

Computer technology affects every field greatly including science and engineering. Development of computer programs has especially contributed to quality of design and analysis. Its application is almost endless from design office to school. Representative softwares are C, C++, Basic, Fortran, MATLAB, etc. Of these, MATLAB offers the best environment, covering not only Matrix Calculation, Industrial Mathematics, Numerical Analysis but also Controlling Theory, Artificial Intelligence, Signal and System as well. By applying coded and programmed design criteria, a designer can easily and effectively perform the given project. In this chapter, a simple but effective automatic designing program will be introduced.

6.2 Description of MATLAB

MATLAB standing for MATrix LABoratory was developed by researchers who joined the Linpack and the Eispack projects. MATLAB was made on the basis of C language by Math Works. When it was first developed, MATLAB was aimed to easily solve matrix calculations, linear algebra, numerical analysis. Currently, it can be applied to calculus, algorithm development, modeling for engineering and science, versatile graphic functions and more. MATLAB is one of the most recommended engineering software programs primarily due to its convenience. If MATLAB is used, a user can avoid difficulties when he/she encounters problems against general and tricky programming languages like Fortran, C, and Pascal. The biggest benefit of MATLAB is that a user can

solve given problems simply and easily by using M–file. This M-file can be written in any editor since it is a text file and it is sorted to Script M–file and Function M–file. Script M-file allows users to write numerous commands and use them at the same time. Meanwhile, Function M–file can be used as a new function.

6.3 Development of Design Program

6.3.1 Programming process

Characteristics of solid round bar connections were shown in the previous chapters. On the basis of this knowledge, an automatic design program was developed using MATLAB codes. This simple and effective program can guide a designer to easy and efficient design. The basic process is explained in Fig.6.1: a flow chart of the design programming, and full codes are shown in Appendix F.

6.3.2 Application and verification

First, when a user runs a coded program or *flange.m*, the program asks the user variables such as service load, material properties, an approximate bolt size and properties of the bolt (refer to Fig.6.2 and Fig.6.3)

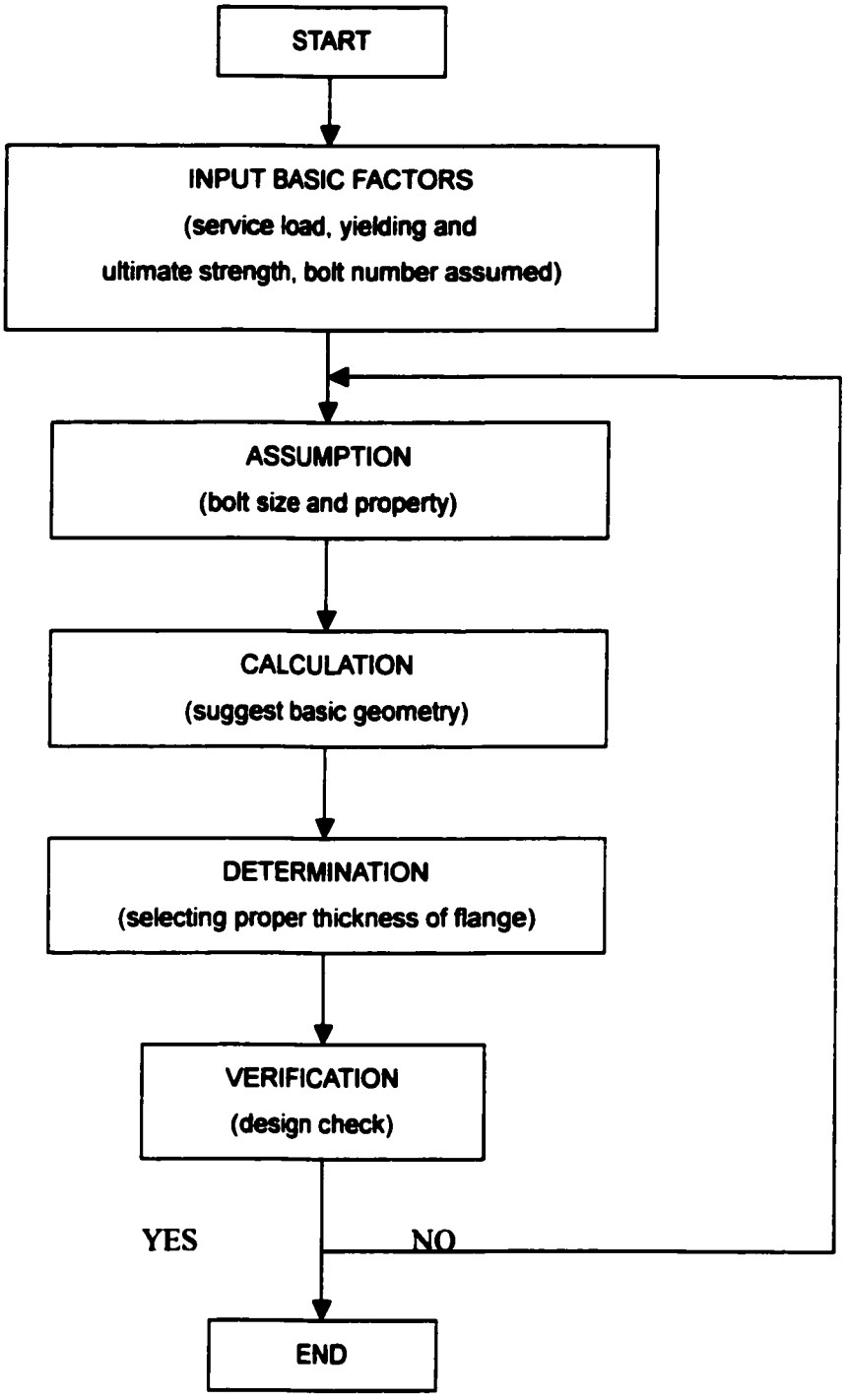

Fig. 6.1 Flow chart of design program

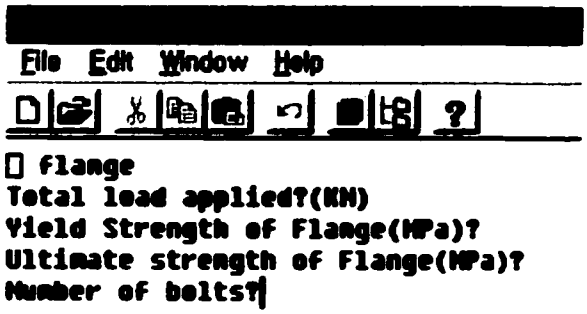

Fig. 6.2 Initial input for the design program

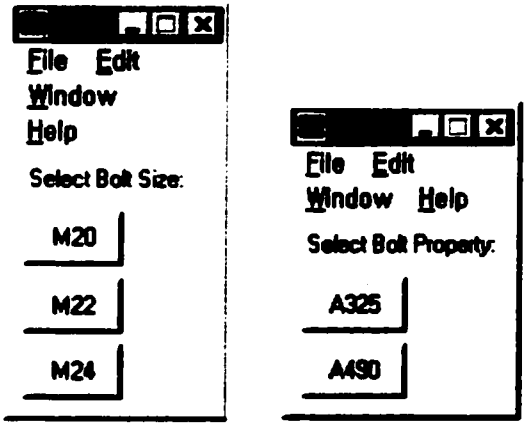

Fig. 6.3 Input about bolt sizes and properties

When a user inputs values asked, the program suggests basic geometry including thickness of a circular flange, and then the design check is also shown (refer to Fig.6.4).

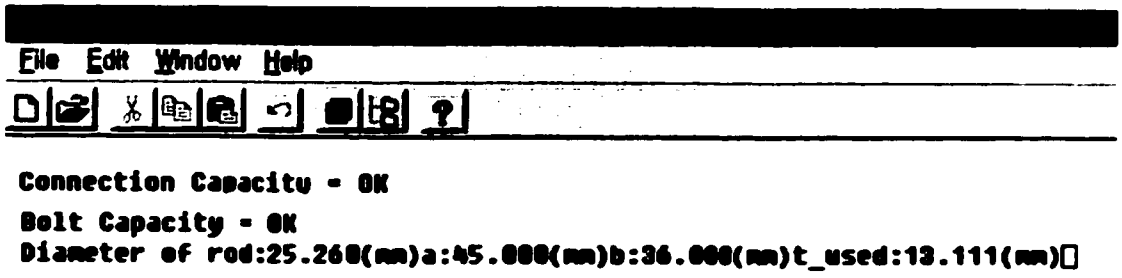

Fig.6.4 Results shown after calculation

In order to verify the result, a sample design in Appendix E was compared with the coded one in Table 6.1. The important value is thickness of a flange, t, and both values, *flange.m* and *sample design*, agreed well.

Table 6.1 Comparison between design program and sample design

	a(mm)	b(mm)	t(mm)	C(kN)	B(kN)
Design program	45.0	36.0	13.11	162.16	71.05
Sample design*	45.0	36.0	13.00	159.50	71.33

*Sample design is shown in Appendix E and the diagram is shown in Chapter II

where,

a = Distance from the edge of the flange to the center of the bolt hole (mm)

b = Distance from the center of bolt hole to the surface of the rod (mm)

t = Flange thickness (mm)

C = Connection capacity (kN)

B = Bolt force (kN)

CHAPTER VII

CONCLUSIONS AND RECOMMENDATIONS

7.1 Summary and Conclusions

The phenomena related to the bolted flange connections were reviewed in this thesis through experimental work and finite element analysis. In the experiment, twelve pairs of circular flanges and twenty-four pairs of bolts and nuts were used. Hand calculation to predict failure agreed very well during the experiment for group 1: rod-failure. Meanwhile, a slight eccentricity effect was observed in group 2, so the bolt failure load was a bit lower than the value calculated manually.

In order to estimate the bolt force, a load cell was used to estimate it by the *force equilibrium method*, indirectly. Because the size of the load cell was big enough to stay in the elastic range, measuring elongation was satisfactory after the bolt was over the elastic until failure. Employing these data, several things were analyzed such as prying force. This load cell was used for the specimen 1 (S-1) in group1 and the strain gages were treated with extreme care owing to their sensitivity. During the experiment, specimen 6 (S-6) in group 1 failed in the threaded section of the bolt so the failure load was lower than that of other specimens. All other bolts in group 2 failed at a certain level of the external load.

Separation of the flanges was measured directly using a digital caliper. Because of slippage, the gap of the flanges was sometimes reduced in group 1, since they were held by

grips, despite external loading but general results were satisfactory. However, proper nuts were used to hold the specimens in group 2 to provide more stable condition. In both group 1 and group 2, asymmetric separation was observed.

In analytical modeling, relatively fine mesh and bilinear reduced integration elements were used. The loading condition was distributed load in the top surfaces of the rods, and plastic material property were given and analyzed. Through the whole analysis, two steps were given: preloading and loading. The results were satisfactory and they were placed in the range between the theoretical and the experimental data.

In order to help engineers in design industry, step-by-step design approaches for a solid rounded bar connection were proposed clearly. Thus, if each step in the guide is followed, the design will be effective and easy. And the general design criteria also were described in Chapter VI. On the basis of this method, a brief and systematic design program was shown using MATLAB codes. By just inputting some values asked for, engineers can easily and reliably obtain basic design data.

According to the analysis, several things were observed below

- Prying force was developed from 60 kN to 135 kN tensile load and its peak ratio, prying force to the external load, was 18% at 105 kN to 120 kN loading ranges.
- Bolt force was calculated using average strain of a load cell and its maximum increase was 40.4 kN at 135 kN tensile load.

- Gap developments were checked in every 30 kN interval and they did not appear symmetrical. Thus, deformed shapes of the flanges were unbalanced in almost all specimens.
- T-stub equivalent equations were applied to solid rounded flange connections and the errors were +16.7% for Eq.2-1 and +18.3% for Eq.2-2, respectively, at 105 kN load. When it comes to conservative design, these equations can be used for not only T-stub but also round bar connections.
- In numerical simulation, continuum solid elements with relatively fine mesh were used.
- Bilinear reduced integration elements showed the satisfactory results.
- The results obtained from the analytical modeling were placed between the theoretical and the experimental values.
- By comparing the bolt failure load by hand calculation, a slight eccentric effect was observed in the round bar connection (failure load expected was 163 kN without eccentricity but it failed at 143 kN, average value). However, in the T-stub case, eccentricity effect was almost negligible despite similar geometries.
- To help engineers in the design industry, systematic design steps were proposed.
- On the basis of the step-by-step design method, an automatic design program employing MATLAB was developed.

7.2 Recommendations for Future Research

More extensive study is needed to investigate phenomena not studied in this thesis including varying contact area, contact force, and eccentricity effect. If enough specimens

are occupied, the effect of different flange thickness under the external load should be studied and the most effective design method must be suggested. Moreover, the optimum design program for a solid round bar connection should be developed for the design industry including a cost estimate. In addition, if possible, more accurate design equations should be developed for solid round bar connections to reduce construction costs.

References

[1] Bick, John H., 1995, **An Introduction to the Design and Behavior of Bolted Joints,** DEKKER

[2] CISC, 2000, **Handbook of Steel Construction** (7^{th} edition), Canadian Institute of Steel Construction

[3] Cao, J. J. and Bell, A. J., 1996, **Determination of Bolt Forces in a Circular Flange Joint under Tension Force**, Int.J.Pres.Ves.&Piping pp.63-71

[4] Cook, R.D., Malkus, D.S., and Plesha, M. E., 1986, **Concept and Applications of Finite Element Analysis** (3^{rd} edition), John Wiley & Sons

[5] Corro, C. L., 1998, **An Evaluation of the Behavior of Slip-Critical Connections Subjected to Combined Shear and Tension**, M.A.Sc Thesis, University of Windsor, Windsor, ON, Canada

[6] H.K.S, 1997, **ABAQUS standard manual**, Hibbitt, Karlsson & Sorensen, Inc.

[7] Kulak, Fisher, and Struik, 1987, **Guide to Design Criteria for Bolted and Riveted Joints**, John Wiley & Sons

[8] Kim, C.G., 1998, **MATLAB and Its Application**, Kyowosa

[9] Kim, S. B. 1985, **Steel Structures**, Kimundang

[10] Salmon & Johnson, 1980, **Steel Structures (Design and Behavior)**, Harper & Row

[11] Sherbourne and Bahaari, 1996, **3D Simulations of Bolted Connections to Unstiffened Columns-I**, J. Construct. Steel Res. Vol.40, No3, pp169-187

[12] Sherbourne and Bahaari, 1996, **3D Simulations of Bolted Connections to**

Unstiffened Columns-II, J. Construct. Steel Res. Vol.40, No3, pp189-223

[13] Smistakidis, E., Baniotopoulos, C. C, Bisbos,C.D., and Panagiotopoulos, P. P., 1997, **Steel T-stub Connections under Static Loading**, J. Construct. Steel Res. Vol.44, No1-2, pp51-67

[14] Swanson, J.A., 1999, **Characterization of the Strength, Stiffness, and Ductility Characteristics of T-Stub Connections**, Ph.D Dissertation, Georgia Institute Technology, USA

[15] Ugural, A.C, and Fenster, S. K., 1995, **Advanced Strength and Applied Elasticity**, Prentice Hall

APPENDIX A

(Dimensions of Flanges)

Appendix A – Dimensions of the flange (group 1)

[mm]

	S1	S2	S3	S4	S5	S6	AVE.	USE	DRAWING
(a)	18.06	16.83	17.55	17.01	17.90	18.81	17.71	17.00	-
	17.02	18.13	16.94	16.10	17.85	18.43			
	16.30	18.39	18.26	17.69	18.26	18.37			
	17.74	17.33	17.56	18.06	18.72	17.79			
(b)	17.62	17.38	17.07	17.50	17.96	17.62	17.68	17.00	-
	17.67	17.47	16.80	17.22	18.01	17.71			
	17.67	17.61	18.47	18.93	18.01	17.86			
	17.64	17.60	17.14	17.57	17.98	17.85			
(c)	88.63	88.43	88.83	88.42	88.42	88.69	88.52	89.00	88.90
	88.56	88.48	87.38	88.87	89.08	88.4			
	88.66	88.44	88.54	88.44	89.13	88.11			
	88.44	88.66	88.00	88.93	88.52	88.30			
(d)	25.47	25.42	25.52	25.40	25.49	25.40	25.70	25.00	-
	26.03	25.58	25.63	26.53	26.12	25.92			
	25.59	25.41	25.70	25.64	25.46	25.60			
	25.48	25.72	25.95	25.85	25.74	26.22			
(e)	43.14	43.53	45.90	45.66	45.36	45.57	44.90	44.00	38.10
	42.82	44.04	45.15	45.76	44.81	45.44			
	46.02	41.95	46.08	43.94	45.65	46.40			
	44.18	43.83	45.71	44.93	43.71	47.92			
(i)	200.20	221.49	220.91	219.16	221.19	222.46	216.94	216.00	203.20
	200.20	223.82	217.78	219.87	224.46	221.22			
	200.20	220.10	222.56	219.99	223.67	223.23			
	200.20	218.85	217.03	203.70	222.92	222.41			
(g)	20.39	19.66	20.64	20.07	19.42	19.45	19.83	19.00	19.05
	19.42	19.24	19.67	19.51	20.36	20.54			
	20.53	19.52	19.47	19.81	19.61	19.53			
	19.81	19.71	19.88	19.94	19.74	20.02			
(h)	28.64	29.27	29.08	29.01	29.76	30.11	29.32	29.00	-
(f)	156.16	177.73	173.86	170.36	178.18	176.00	172.04	172.00	165.90

Refer to Fig.3.1

Appendix A – Dimensions of the flange (group 1)

[mm]

	F1	F2	F3	F4	F5	F6	AVE.	USE	DRAWING
(a)	20.22	20.28	19.46	20.05	19.95	20.10	20.14	20.00	-
	21.19	21.27	19.76	19.67	19.89	21.16			
	20.12	20.50	19.90	19.64	19.82	20.50			
	20.45	20.66	20.04	19.56	19.75	19.63			
(b)	15.39	15.84	16.81	17.09	17.01	16.33	16.41	17.00	-
	15.35	16.32	16.96	16.89	17.04	16.81			
	15.41	16.19	17.29	16.87	16.12	15.77			
	15.36	16.20	16.38	17.15	17.30	16.15			
(c)	88.43	88.41	88.23	88.59	88.59	88.62	88.52	89.00	88.90
	88.82	88.02	88.80	88.76	88.77	88.41			
	88.80	88.48	88.13	88.63	88.51	88.48			
	89.29	87.65	89.15	88.23	88.49	88.25			
(d)	38.13	38.24	38.25	38.33	38.13	38.13	38.30	38.00	-
	38.27	38.26	38.61	38.25	38.22	39.14			
	38.40	38.23	38.28	38.27	38.30	38.15			
	38.31	38.33	38.25	38.18	38.13	38.71			
(e)	52.98	52.51	52.79	52.27	53.26	52.47	52.54	52.00	-
	52.15	52.70	52.93	52.02	51.71	53.48			
	50.56	51.89	53.14	52.42	53.15	52.69			
	52.89	52.69	52.67	52.97	53.14	51.73			
(i)	305.19	297.78	302.63	304.68	303.52	296.64	301.58	301.00	-
	303.30	293.41	304.50	306.15	304.69	306.17			
	306.75	299.61	303.28	289.62	302.94	291.45			
	302.86	301.43	303.95	299.18	305.44	302.90			
(g)	19.53	20.30	21.23	19.52	19.68	19.41	20.15	20.00	19.05
	19.58	20.55	21.11	19.75	19.08	21.09			
	19.51	21.12	19.43	20.11	21.32	19.27			
	19.63	21.27	19.59	19.81	21.00	20.93			
(h)	28.17	28.73	28.22	28.23	28.28	28.47	28.35	28.50	-
(f)	252.38	245.61	250.71	247.48	251.33	246.70	249.03	249.00	-

Refer to Fig.3.1

APPENDIX B

(Detailed Calculations)

Appendix B

Detailed calculation for measuring bolt stiffness

$$\frac{1}{K_B} = \frac{L_{BA}}{EA_B} + \frac{L_{Se}}{EA_S} \qquad (4\text{-}1)$$

where,

K_B = Stiffness of the bolt (MN/m)

E = Young's Modulus

L_{Be} = Effective length of the body (m)

A_B = Cross sectional area of the body (m^2)

L_{Se} = Effective length of the thread (m)

A_S = Cross sectional area of the thread (m^2)

Detailed diagram shown in Fig3.2

Nominal body diameter (D) = $15.8 * 10^{-3}$ m

Nominal shank diameter (L) = $69 * 10^{-3}$ m

$A_B = \pi/4*D\text{^}2 = \pi/4* (15.8*10^{-3})\text{^}2 = 196 * 10^{-6}$ m^2

$L_B = L - L_T = 0.069\text{-}0.044 = 25 * 10^{-3}$ m

A_S = 5/8" –24 = $173 * 10^{-6}$ m^2

$L_{Be} = L_B + T_H/2 = 0.025 + 0.012 / 2 = 31* 10^{-3}$ m

$L_{Se} = L_G - L_B + T_N/2 = 0.038 - 0.025 + 0.015/2 = 20.5 * 10^{-3}$ m

$1/K_B = L_{Be} / EA_B + L_{se} / EA_S$

$= (31 * 10^{-3}) / (317.5*10^9 * 196 * 10^{-6}) + (20.5 * 10^{-3})/ (317.5*10^9 * 173 * 10^{-6})$

Therefore,

K_B = 1,147 MN/m

Appendix B

Detailed calculation for Eq.2-1

$K = 4b' 10^3 / (\Phi p F_y)$
$= 4*39*10^3 / (0.9*58*385) = 7.762$

where,

$b' = b - d/2 = 47-16/2 = 39mm$

$\Phi = 0.9$

$p = 29*2 = 58mm$ (diameter of effective cylinder proposed)

$F_y = 385MPa$

$\delta = 1 - d' / p = 1 - 18 / 58 = 0.69$

$\alpha = (K P_f / t^2 - 1) * 1/ \delta = (7.762 * P_f / 19^2 - 1) * 1 / 0.69 = 0.03 P_f - 1.45$

$$T_f = P_f[1 + (\frac{b'}{a'} \times \frac{\delta\alpha}{1 + \delta\alpha})] \qquad (2\text{-}1)$$

$T_f = P_f[1 + (38 / 38) * (0.69 * (0.03 P_f - 1.45)) / (1 + 0.69*(0.03 P_f - 1.45))]$
$= P_f [1+ (0.0207 P_f - 1) / (1 + 0.0207 P_f - 1)]$
$= 2 P_f - 48.31$

e.g.) External load = 105KN→ bolt force = 2 * 105 – 48.31 = 161.69KN

**Remark

1) Detailed descriptions are referred to ref.9, p.3-20

Appendix B

Detailed calculation for Eq.2-2

- Given factors

S = tool scatter = 0.30, $e_m = 0.1$, $e_{EI} = 0.18$

F_{pa} = target preload = 110KN, n = loading plane factor = 0.5

- Joint

$E = 192.5GPa$, $a = 0.089/2 = 0.0445$, $s = 0.089/2 - 0.029 = 0.0155$

$L_G = T = 0.019 * 2 = 0.038$, T_{min} = thickness of thinner joint member = 0.019

b = distance between bolts = 0.029*2=0.058 (diameter of effective cylinder proposed)

$w = D_J = 0.089 - 0.26 / 2 = 0.76$

- Bolt

$A_s = 173 * 10^{-6}\ m^2$, $E = 317.5GPa$, $K_B = 1147 * 10^6\ N/m$

$\sigma_y = 635\ MPa$, D_B = width across flats of the head of the bolt = 0.022m, $D_H = 0.018m$

$A_J = b * (D_B + T_{min}) = 0.058 * (0.022 + 0.019) = 0.0024$

$A_c = \pi / 4\ [(D_B + T/10)^2 - D_H] = \pi /4\ [(0.022 + 0.038 /10)^2 - 0.018^2] = 268 * 10^{-6}$

$R_G = d/2 = (0.089*2) / 2 = 0.089$

$K_{JC} = E A_c / T = (192.5 * 10^{9)} * 268 * 10^{-6} / 0.038 = 1357 * 10^6$

$r_J = 1 / K_{JC} = 1.0$

$\lambda^2 = s^2 A_c / (R_G^2 A_J) = 0.0155^2 * 268*10^{-6} / (0.089^2 * 0.0024) = 3386 * 10^{-6}$

$r_J' = r_J(1 + \lambda^2) = 1\ (1 + 3386 * 10^{-6}) = 1.0034$

$r_J'' = r_J(1 + (a\lambda^2/s)) = 1\ (1 + (0.0445 * 3386 * 10^{-6}/ 0.0155)) = 1.0097$

$r_B = 1 / K_B = 1 / (1147 * 10^2) = 8.71 * 10^{-10}$

$K_J'' = 1 / r_J'' = 1 / 1.0097 = .995$

$\Phi_{cn} = n\ (r_J'' / (r_J' + r_B)) = 0.5 * (1.0097 / (1.0034 + 8.71 * 10^{-10})) = 0.50$

$$F_B = (1 + s) F_{pa} - \Delta F_m - \Delta F_{EI} + \Phi_{cn} L_x \qquad (2\text{-}2)$$

$F_B = (1 + 0.3) * 110 - 0.1 * 110 - 0.18 * 110 + 0.50 * L_x$

$= 112.2 + 0.50\ L_x$ [KN]

e.g.) external load = 105KN→ $112.2 + 0.50 * 105 = 164.70$KN

**Remark

1) Detailed descriptions are referred to ref.1, p.496

APPENDIX C

(Experimental Data)

Appendix C

Sample 1 (S-1)											
Strain (10^{-6})	External Load (kN)										
	0	30	60	90	120	150	180	210	240	270	276
#1	0.00	-8.00	-19.00	-23.00	-93.00	-184.00	-281.00	-374.00	-545.00	-755.00	-835.00
#2	0.00	-7.00	-12.00	-24.00	-86.00	-164.00	-254.00	-327.00	-394.00	-465.00	-487.00
#3	0.00	-10.00	-22.00	-43.00	-147.00	-265.00	-430.00	-631.00	-779.00	-933.00	-967.00
#4	0.00	-9.00	-17.00	-31.00	-94.00	-170.00	-234.00	-301.00	-385.00	-478.00	-494.00
#5	0.00	3.00	1.00	0.00	-51.00	-114.00	-185.00	-282.00	-429.00	-589.00	-621.00
#6	0.00	1.00	-5.00	-7.00	-81.00	-173.00	-258.00	-361.00	-523.00	-698.00	-737.00
#7	0.00	-4.00	-5.00	-9.00	-79.00	-159.00	-253.00	-310.00	-350.00	-409.00	-431.00
#8	0.00	-3.00	-7.00	-13.00	-98.00	-205.00	-329.00	-469.00	-585.00	-677.00	-687.00
Average	0.00	-4.63	-10.75	-18.75	-91.13	-179.25	-278.00	-381.88	-498.75	-625.50	-657.38

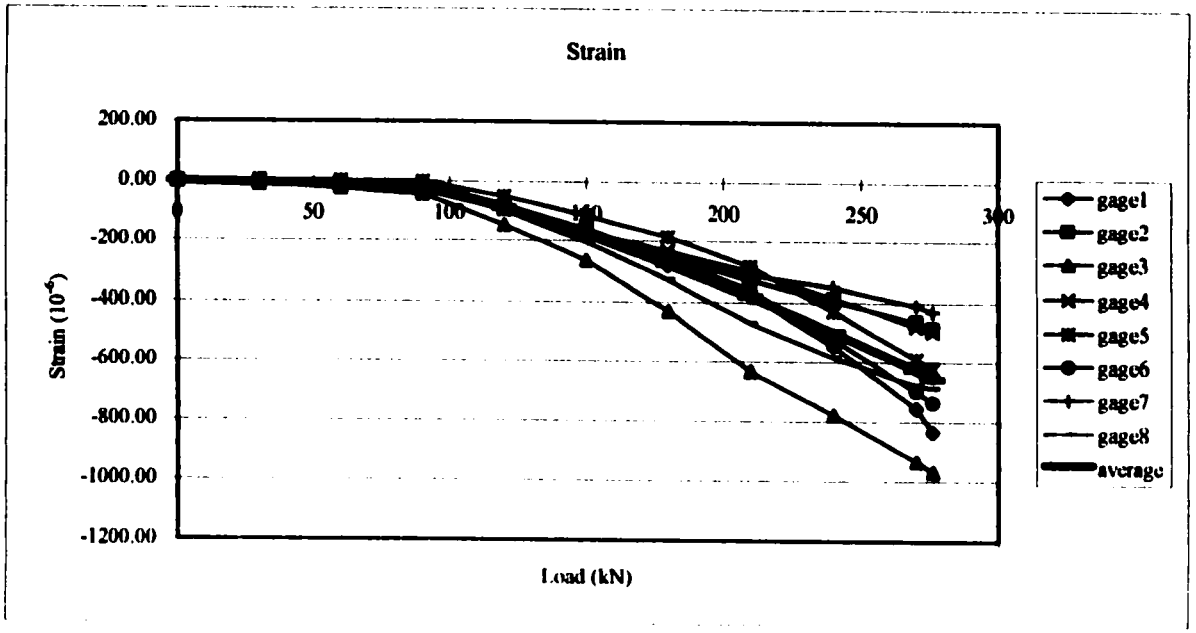

Appendix C

Sample 1 (S-1)												
Gap(mm)		External Load (kN)										
Marker	Location	0	30	60	90	120	150	180	210	240	270	276
#1	0.074	0.00	0.00	-0.34	-0.11	0.45	0.70	0.11	3.51	1.99	2.77	
#2	0.039	0.00	0.00	0.86	0.76	-0.24	0.36	0.75	-0.32	0.51	-0.18	
#3	-0.039	0.00	0.00	-0.18	-0.07	-0.46	-0.01	1.06	2.32	2.36	3.15	
#4	-0.074	0.00	0.00	0.32	1.42	0.31	0.38	0.49	0.62	0.80	0.70	
#5	0.074	0.00	-1.36	0.38	-0.85	-0.80	-0.33	-0.07	1.18	1.63	2.39	
#6	0.039	0.00	-0.83	-0.54	0.51	-0.47	0.56	-0.18	-0.47	-0.55	-0.11	
#7	-0.039	0.00	-0.01	-0.67	-0.31	-0.22	-0.99	1.37	2.04	3.03	2.56	
#8	-0.074	0.00	-0.55	1.04	1.27	-0.16	-0.52	0.07	-1.29	-1.16	-1.31	fail

Group 1 (S-1): Diagonal 1

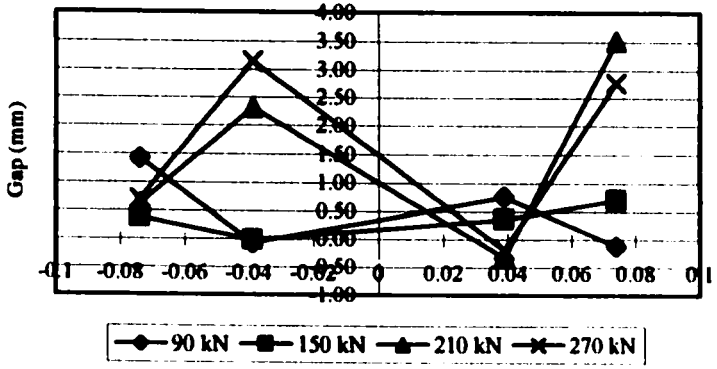

Group 1 (S-1): Diagonal 2

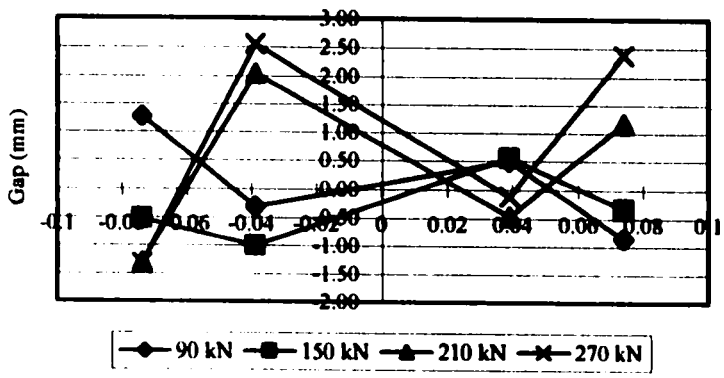

Appendix C

Sample 2 (S-2)												
Gap(mm)		External Load (kN)										
Marker	Location	0	30	60	90	120	150	180	210	240	270	274
#1	0.074	0.00	2.88	3.17	3.53	3.26	3.18	3.32	3.78	3.33	2.13	
#2	0.039	0.00	2.28	2.73	2.27	2.88	2.31	2.63	2.88	2.09	2.25	
#3	-0.039	0.00	1.87	2.43	3.12	2.38	2.20	2.84	2.93	1.78	1.72	
#4	-0.074	0.00	1.94	2.03	2.38	2.45	2.14	2.99	2.81	2.40	2.23	
#5	0.074	0.00	1.19	0.83	1.93	1.59	1.35	2.31	2.06	2.57	3.27	
#6	0.039	0.00	0.73	0.82	1.45	1.26	1.00	1.96	2.13	2.32	3.39	
#7	-0.039	0.00	1.57	0.90	0.99	0.86	1.00	1.92	1.87	1.68	2.42	
#8	-0.074	0.00	1.14	1.43	1.07	1.25	1.57	2.03	2.24	2.55	3.08	fail

Group 1 (S-2): Diagonal 1

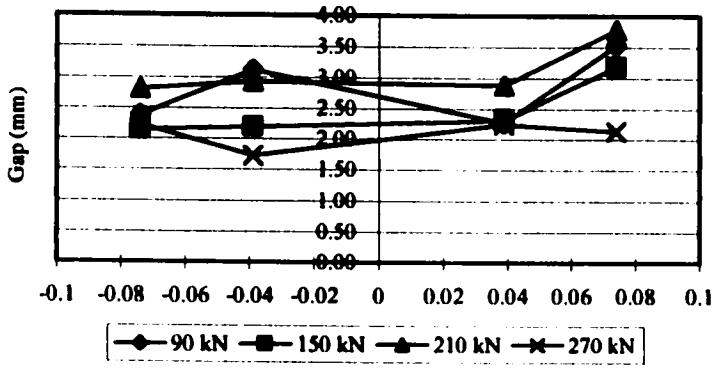

Group 1 (S-2): Diagonal 2

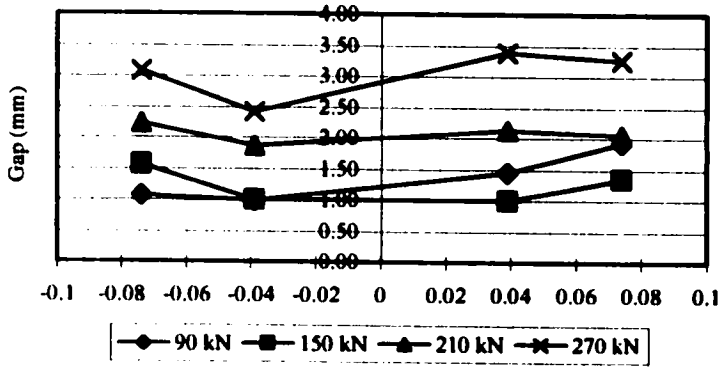

Appendix C

Sample 3 (S-3)												
Gap(mm)		External Load (kN)										
Marker	Location	0	30	60	90	120	150	180	210	240	270	281
#1	0.074	0.00	-0.14	0.22	0.24	1.87	1.04	0.71	1.21	1.06	1.43	
#2	0.039	0.00	0.10	-0.22	0.35	-0.27	-0.08	-0.05	0.49	0.67	1.55	
#3	-0.039	0.00	-0.21	-0.46	-0.52	0.11	0.82	-0.07	-0.18	0.07	0.69	
#4	-0.074	0.00	-0.21	-0.40	-0.29	-0.42	0.49	-0.31	0.25	-0.07	0.84	
#5	0.074	0.00	-0.60	-0.19	-0.58	-0.09	0.26	-0.09	0.21	0.66	1.77	
#6	0.039	0.00	-0.35	-0.23	-0.48	0.02	-0.18	-0.50	1.64	0.28	1.20	
#7	-0.039	0.00	-0.52	0.38	-0.59	-0.49	1.05	0.45	0.83	3.26	1.74	
#8	-0.074	0.00	0.15	0.11	-0.19	-0.08	1.16	0.53	1.43	2.87	1.20	fail

Group 1 (S-3): Diagonal 1

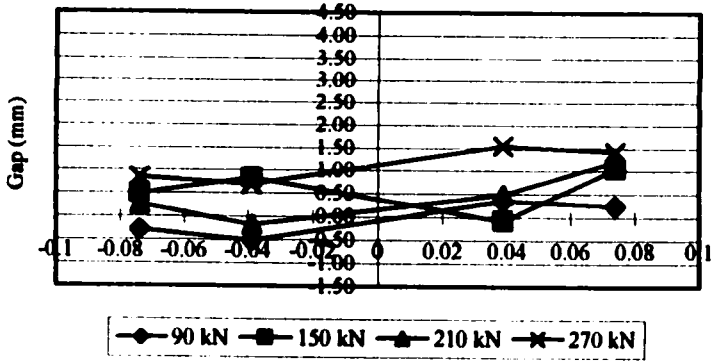

Group 1 (S-3): Diagonal 2

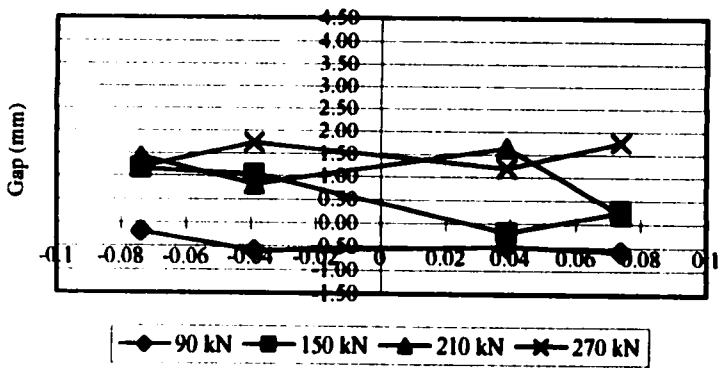

Appendix C

Sample 4 (S-4)												
Gap(mm)		External Load (kN)										
Marker	Location	0	30	60	90	120	150	180	210	240	270	282
#1	0.074	0.00	0.05	0.24	0.54	0.89	0.69	0.81	1.99	2.83	2.94	
#2	0.039	0.00	0.46	0.67	0.71	0.68	0.14	0.88	1.14	2.49	3.81	
#3	-0.039	0.00	-0.39	-0.32	-0.27	0.25	-0.11	-0.52	-0.37	0.23	0.06	
#4	-0.074	0.00	0.10	0.18	0.09	0.80	-0.07	-0.15	0.01	1.19	0.27	
#5	0.074	0.00	-0.86	0.08	-0.40	-0.26	-0.62	-0.52	-0.27	1.50	0.99	
#6	0.039	0.00	0.56	0.42	0.90	0.88	0.18	0.44	0.97	1.27	1.84	
#7	-0.039	0.00	-0.17	-0.01	-0.59	0.95	0.00	0.42	1.36	1.82	3.73	
#8	-0.074	0.00	0.35	0.50	0.70	0.45	0.34	0.71	2.17	2.55	2.87	fail

Group 1 (S-4): Diagonal 1

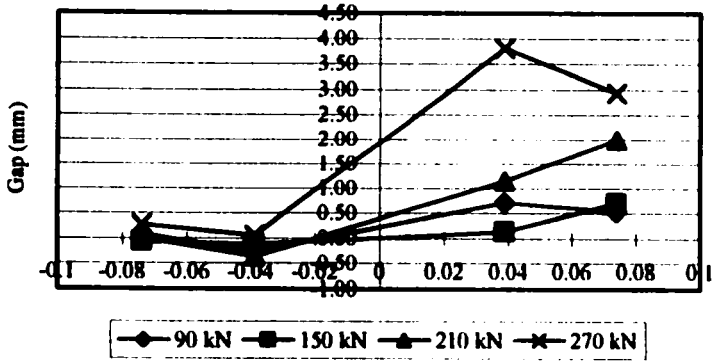

Group 1 (S-4): Diagonal 2

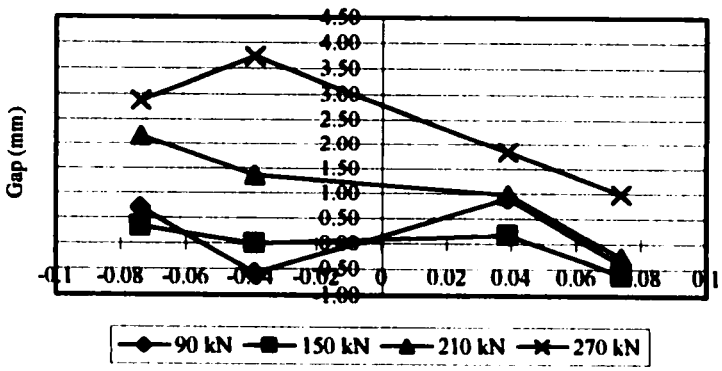

Appendix C

Sample 5 (S-5)												
Gap(mm)		External Load (kN)										
Marker	Location	0	30	60	90	120	150	180	210	240	270	276
#1	0.074	0.00	-0.13	-0.26	-0.64	-0.56	0.23	-0.23	-0.82	-0.42	-0.61	
#2	0.039	0.00	-0.97	-0.80	-0.68	-1.34	-1.23	-0.49	-0.77	-0.15	-0.39	
#3	-0.039	0.00	0.69	0.87	-0.04	0.42	1.33	2.02	1.36	3.45	3.05	
#4	-0.074	0.00	0.84	0.42	0.75	0.70	2.04	2.43	2.35	3.15	3.79	
#5	0.074	0.00	0.68	-0.43	0.15	0.38	0.32	0.71	1.35	1.85	2.42	
#6	0.039	0.00	0.01	-0.20	-0.17	0.23	0.15	0.35	0.89	0.86	2.58	
#7	-0.039	0.00	0.73	0.36	0.87	0.58	0.73	0.64	1.23	1.16	0.55	
#8	-0.074	0.00	0.85	0.30	0.36	1.13	1.07	1.60	1.70	2.07	1.20	fail

Group 1 (S-5): Diagonal 1

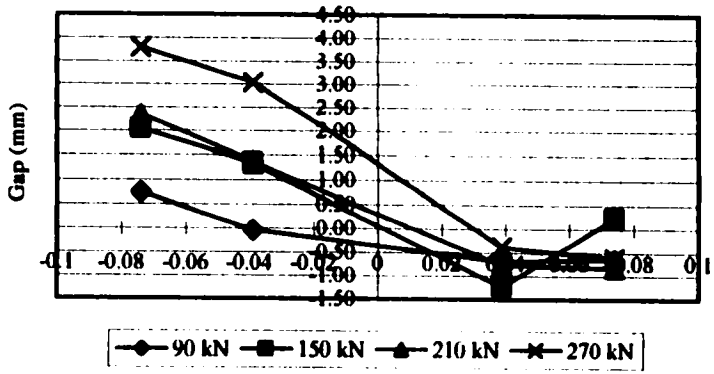

Group 1 (S-5): Diagonal 2

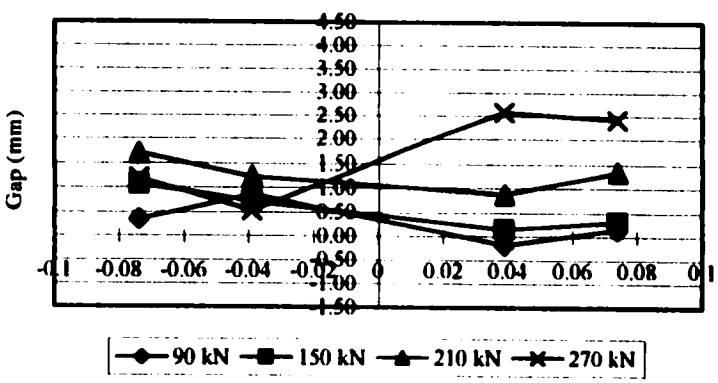

Appendix C

Sample 6 (S-6)												
Gap(mm)		External Load (kN)										
Marker	Location	0	30	60	90	120	150	180	210	240	270	230
#1	0.074	0.00	-0.94	-0.61	-0.67	-0.05	-0.16	-0.49	-0.70	#VALUE!	#VALUE!	
#2	0.039	0.00	-0.21	0.45	0.02	0.65	0.03	0.87	-0.23	#VALUE!	#VALUE!	
#3	-0.039	0.00	0.20	0.66	1.44	0.53	0.94	1.05	0.15	#VALUE!	#VALUE!	
#4	-0.074	0.00	-0.73	0.27	-0.08	0.21	0.07	2.22	0.46	#VALUE!	#VALUE!	
#5	0.074	0.00	-0.62	-0.08	-0.01	-0.17	0.31	0.23	1.68	#VALUE!	#VALUE!	
#6	0.039	0.00	-0.79	-0.01	0.20	0.44	0.55	0.43	1.12	#VALUE!	#VALUE!	
#7	-0.039	0.00	0.94	-0.24	0.12	0.83	1.22	1.98	2.11	#VALUE!	#VALUE!	
#8	-0.074	0.00	-0.32	-0.26	-0.01	0.25	0.52	1.25	1.66	#VALUE!	#VALUE!	fail

Group 1 (S-6): Diagonal 1

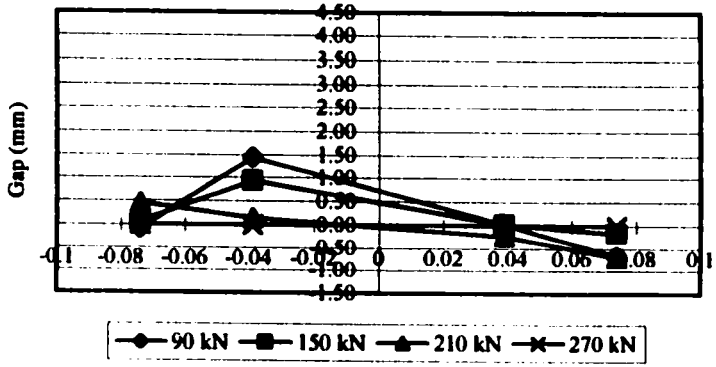

Group 1 (S-6): Diagonal 2

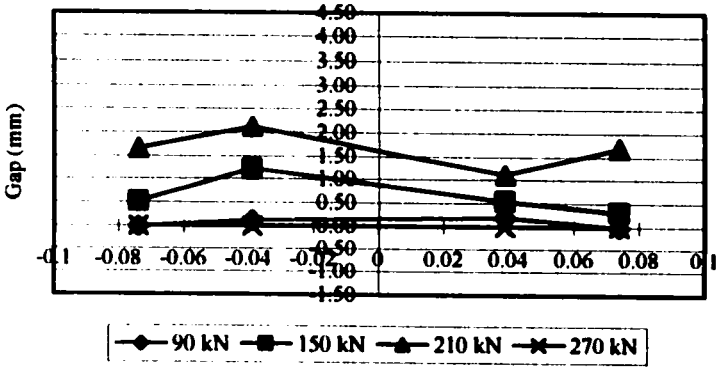

Appendix C

Sample 1 (F-1)												
Gap(mm)		External Load (kN)										
Marker	Location	0	30	60	90	120	150	180	210	240	270	288.8
#1	0.074	0.00	0.16	-0.22	0.80	-0.15	-0.24	-0.86	-0.11	-0.24	0.32	
#2	0.039	0.00	0.03	0.87	1.52	0.90	1.47	1.27	0.77	1.21	1.44	
#3	-0.039	0.00	0.52	0.60	0.28	-0.47	0.95	0.62	0.59	0.63	1.45	
#4	-0.074	0.00	0.38	0.92	0.52	0.18	0.81	0.96	0.79	1.31	1.22	fail

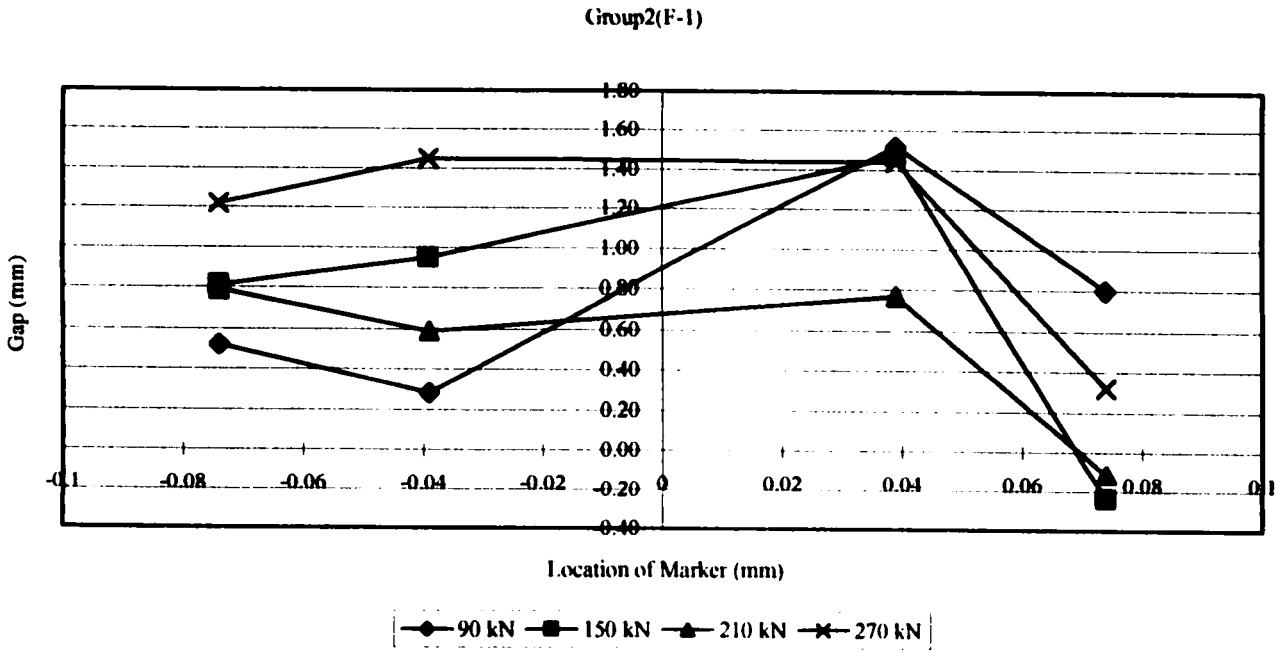

Appendix C

Sample 1 (F-2)												
Gap(mm)		External Load (kN)										
Marker	Location	0	30	60	90	120	150	180	210	240	270	284.5
#1	0.074	0.00	-0.13	-0.37	-1.59	-0.01	-1.61	-1.58	-0.69	-0.57	-1.09	
#2	0.039	0.00	-0.76	-0.05	-0.59	-0.30	0.09	-0.02	0.16	0.60	-0.30	
#3	-0.039	0.00	-0.03	0.10	-0.15	0.91	0.52	0.92	1.57	0.95	1.25	
#4	-0.074	0.00	0.04	0.35	1.49	1.01	1.11	0.85	1.20	2.38	2.38	fail

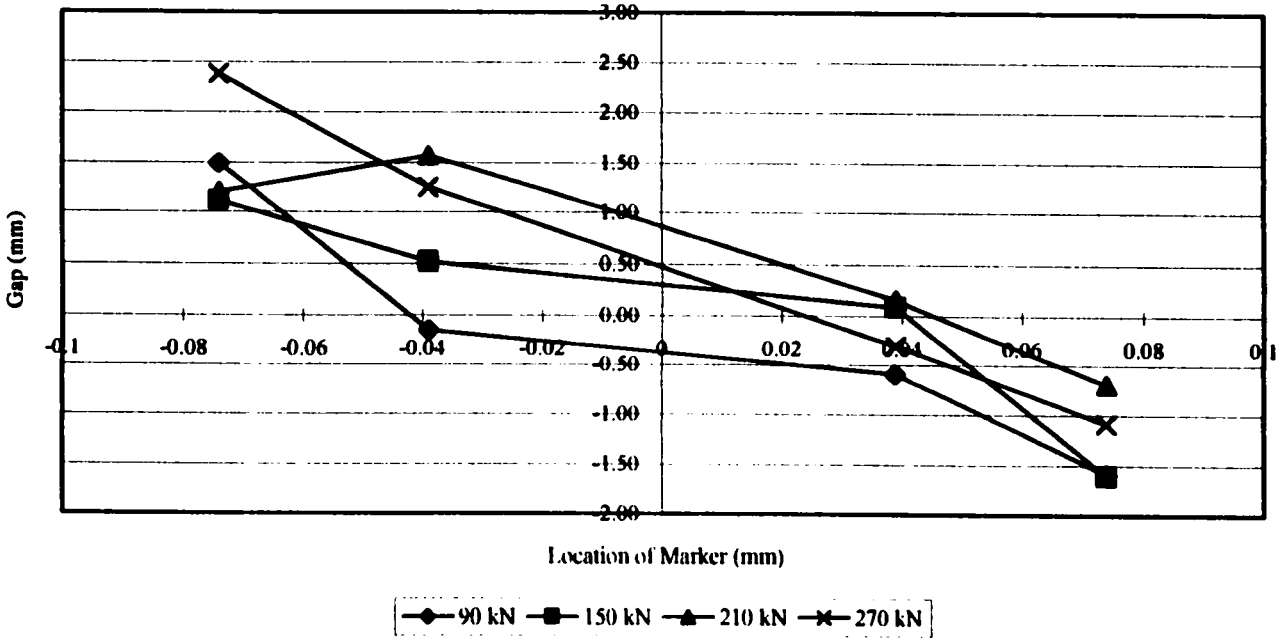

Appendix C

Sample 1 (F-3)												
Gap(mm)		External Load (kN)										
Marker	Location	0	30	60	90	120	150	180	210	240	270	293
#1	0.074	0.00	0.73	-0.65	0.88	0.17	0.23	-0.85	-0.11	0.12	0.08	
#2	0.039	0.00	0.80	0.22	-0.59	-0.11	-0.53	-0.11	0.46	-0.67	0.04	
#3	-0.039	0.00	0.65	0.45	1.10	0.69	-0.79	1.46	0.71	0.30	0.03	
#4	-0.074	0.00	-0.49	-0.67	0.40	-0.89	-0.96	-2.12	-0.12	-1.06	-0.26	fail

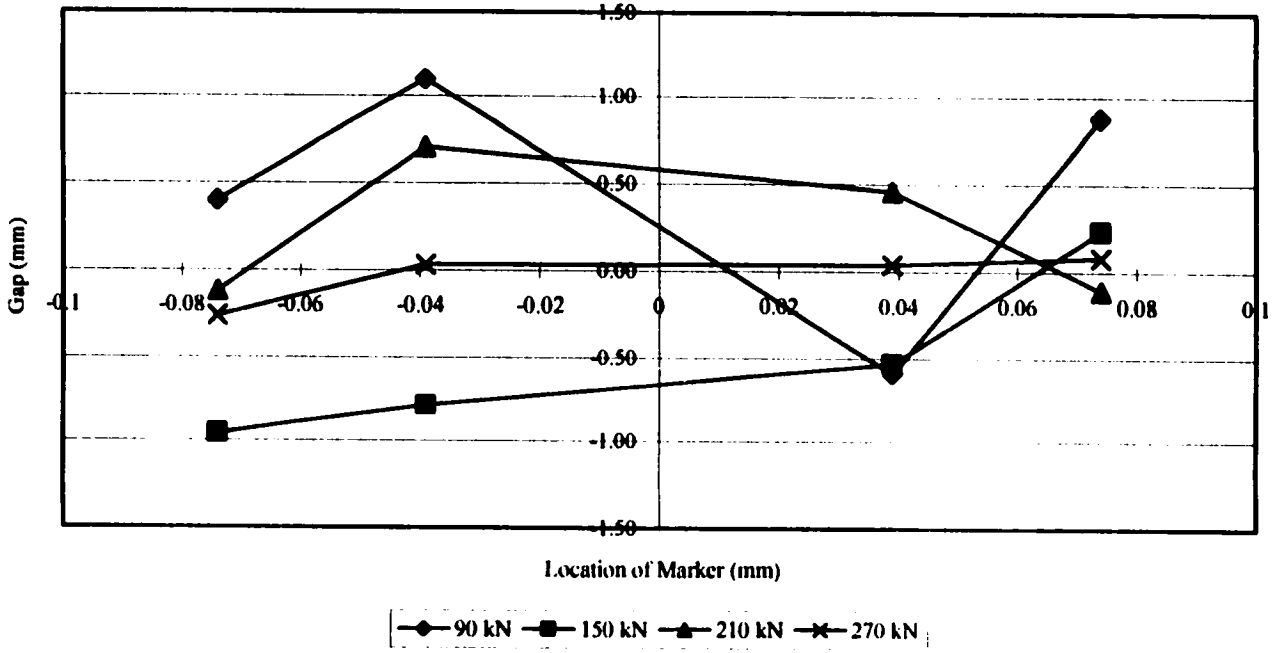

Appendix C

Sample 1 (F-4)												
Gap(mm)		External Load (kN)										
Marker	Location	0	30	60	90	120	150	180	210	240	270	286.8
#1	0.074	0.00	-0.65	-0.98	-0.70	-0.69	-0.97	-1.12	-1.95	-1.17	-1.01	
#2	0.039	0.00	-0.77	0.28	0.94	0.05	-0.51	-0.43	-0.67	0.19	-0.45	
#3	-0.039	0.00	0.00	0.27	-0.64	0.13	-0.05	-1.29	-0.06	-0.87	-0.59	
#4	-0.074	0.00	-0.06	0.44	0.86	0.66	-0.07	0.22	0.68	1.42	0.64	fail

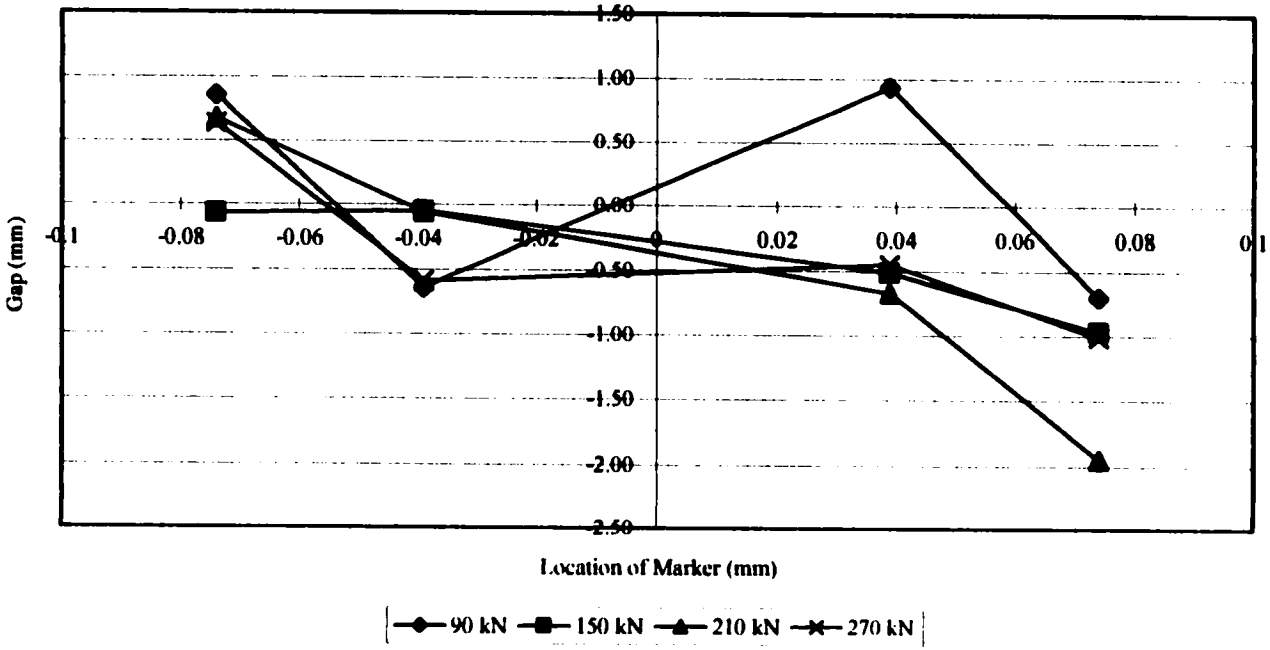

Appendix C

Sample 1 (F-5)												
Gap(mm)		External Load (kN)										
Marker	Location	0	30	60	90	120	150	180	210	240	270	282.5
#1	0.074	0.00	-0.09	-0.43	-0.20	-0.68	0.22	-0.97	-1.08	0.24	0.57	
#2	0.039	0.00	0.96	0.50	0.57	0.67	1.12	0.91	0.42	0.56	0.84	
#3	-0.039	0.00	0.29	0.41	-0.10	1.21	0.08	0.65	1.11	0.82	1.50	
#4	-0.074	0.00	0.64	0.56	0.09	1.15	1.08	0.80	0.72	0.98	1.15	fail

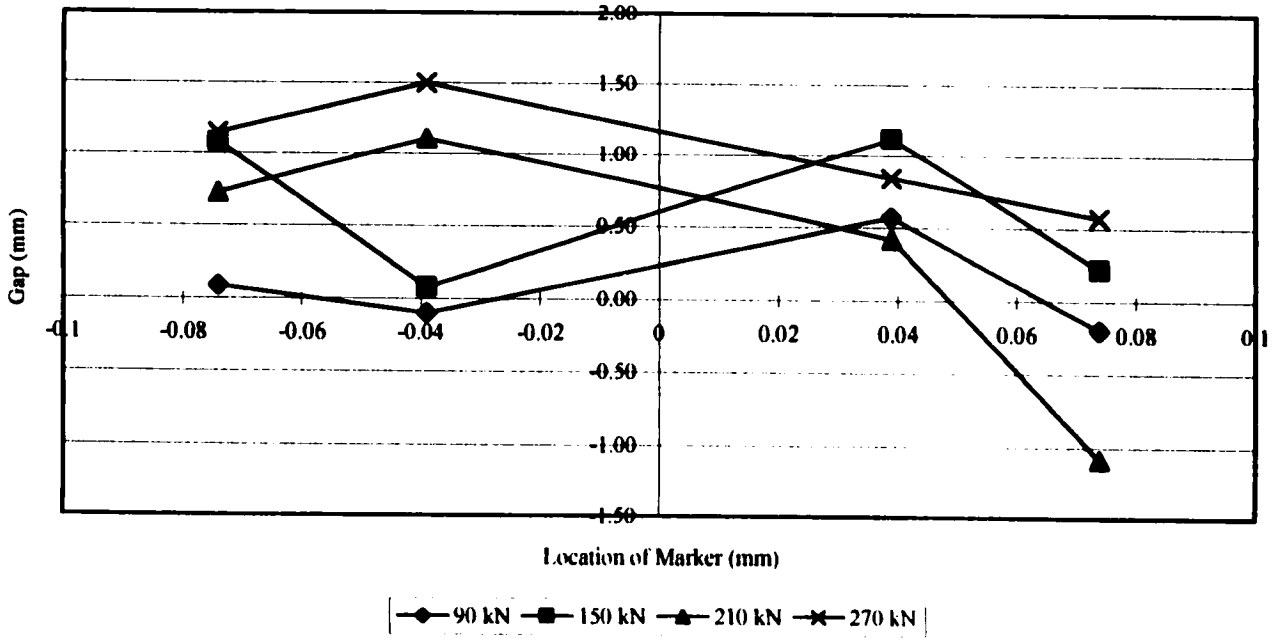

Appendix C

Sample 1 (F-6)												
Gap(mm)		External Load (kN)										
Marker	Location	0	30	60	90	120	150	180	210	240	270	287.9
#1	0.074	0.00	0.09	0.41	-0.83	-0.69	0.21	-0.12	-0.87	-0.05	0.45	
#2	0.039	0.00	0.68	-0.67	-0.57	-0.41	0.31	-0.16	-0.34	-0.24	0.55	
#3	-0.039	0.00	-0.04	0.02	-0.97	0.11	-0.82	-0.80	-1.04	-0.05	0.26	
#4	-0.074	0.00	-0.24	-0.17	-1.36	-0.62	0.61	-1.04	-0.51	-0.52	-0.02	fail

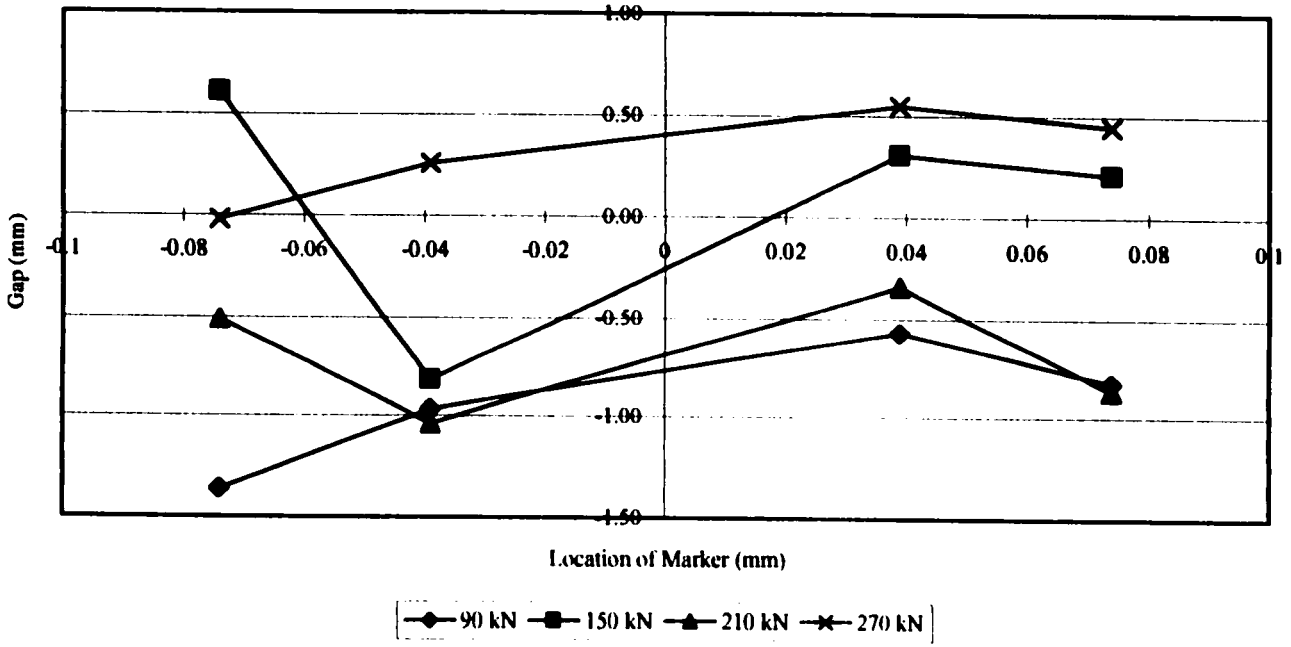

APPENDIX D

(Finite Element Analysis Data)

APPENDIX D
(Strain check in the load cell)

```
*Heading
 Cell_hole
** Job name: cell_hole Model name: Model-1
**
** PARTS
**
*Part, name=Cell
*End Part
**
** ASSEMBLY
**
*Assembly, name=Assembly
**
*Instance, name=Cell-1, part=Cell
*Node
        1.          0.017.          0.,          0.025
        2.          0.026.          0.,          0.025
        3.         -0.026.          0.,          0.025
        4.         -0.017.          0.,          0.025
        5.          0.026.          0.,             0.
         ...
         ...
  176.   -0.0137533.   -0.00999235.          0.01
    177.    0.0137533.   -0.00999235.          0.005
    178.   0.00525329.    -0.016168.          0.005
    179.  -0.00525329.    -0.016168.          0.005
    180.   -0.0137533.   -0.00999235.          0.005
*Element, type=C3D8R
 1.  36.  41. 101.  85.   1.   2.  13.  20
 2.  85. 101. 102.  86.  20.  13.  14.  19
 3.  86. 102. 103.  87.  19.  14.  15.  18
 4.  87. 103. 104.  88.  18.  15.  16.  17
 5.  88. 104.  40.  29.  17.  16.   3.   4
        ...
```

```
          ...
  96.     5.     8.    84.    72.    44.    33. 177. 161
  97.    72.    84.    83.    71. 161. 177. 178. 162
  98.    71.    83.    82.    70. 162. 178. 179. 163
  99.    70.    82.    81.    69. 163. 179. 180. 164
 100.    69.    81.     7.     6. 164. 180.    32.    37
** Region: (Cell:Picked)
*Elset, elset=_I1, internal, generate
   1, 100,     1
** Section: Cell
*Solid Section, elset=_I1, material=Steel
1.,
*End Instance
*Nset, nset=_G13, internal, instance=Cell-1
   1, 11
*Nset, nset=_G15, internal, instance=Cell-1
 169,
*Nset, nset=numerical, instance=Cell-1
 9,
*Elset, elset=__G6_S2, internal, instance=Cell-1
   1,    2,    3,    4,    5, 26, 27, 28, 29, 30, 51, 52, 53, 54, 55, 76
 77, 78, 79, 80
*Surface, type=ELEMENT, name=_G6, internal
__G6_S2, S2
*Elset, elset=__G7_S1, internal, instance=Cell-1
 21, 22, 23, 24, 25, 96, 97, 98, 99,100
*Surface, type=ELEMENT, name=_G7, internal
__G7_S1, S1
*End Assembly
**
** MATERIALS
**
*Material, name=Steel
*Elastic
 2.13e+11, 0.3
**
```

```
** BOUNDARY CONDITIONS
**
** Name: BC-1 Type: Displacement/Rotation
*Boundary
_G13. 1. 1
_G13. 2. 2
_G13. 3. 3
** Name: Numerical Type: Displacement/Rotation
*Boundary
_G15. 1. 1
_G15. 2. 2
_G15. 3. 3
** ----------------------------------------------------------------
**
** STEP: Load
**
*Step. name=Load
Loading pressure
*Static
0.1. 1.. 1e-05. 1.
**
** BOUNDARY CONDITIONS
**
** Name: BC-1 Type: Displacement/Rotation
*Boundary. op=NEW
_G13. 1. 1
_G13. 2. 2
** Name: Numerical Type: Displacement/Rotation
*Boundary. op=NEW
_G15. 1. 1
_G15. 2. 2
_G15. 3. 3
**
** LOADS
**
** Name: Load      Type: Pressure
```

```
*Dsload
_G6. P. 1.7e+08
** Name: Load_Dn      Type: Pressure
*Dsload
_G7. P. 4.45e+08
**
** OUTPUT REQUESTS
**
*Restart. write. frequency=1
**
** FIELD OUTPUT: F-Output-1
**
*Output. field
*Element Output
S. E
*Output. history. frequency=0
*El Print. freq=999999
*Node Print. freq=999999
*End Step
```

APPENDIX D
(Typical input for flange analysis)

```
*Heading
  Analysis of bolted flange connections under tensile loading
**
** PARTS
**
*Part, name=Bolt
*End Part
*Part, name=Fl_Dn
*End Part
*Part, name=Fl_Up
*End Part
*Part, name=loadcell
*End Part
**
** ASSEMBLY
**
*Assembly, name=Assembly
**
*Instance, name=Bolt-1, part=Bolt
0.001, 0.06, -5.55112e-17
0.001, 0.06, -5.55112e-17, 1.001, 0.06, 4.11708e-16, 90.
*Node
        1.          0.005.          0.019.          0.
        2.         -0.005.          0.019.          0.
        3.          0.008.          0.019.          0.
        4.         -0.008.          0.019.          0.
        5.          0.008.         -0.0125.         0.
        ...
        ...
    1630.  -0.00511863.          0.0255.   0.00614814
    1631.  -0.00242588.          0.0255.   0.00762333
    1632.  0.000746138.          0.0255.   0.00796513
    1633.   0.00425174.          0.0255.   0.00677663
```

```
    1634.     0.00697343.          0.0255.     0.00392062
*Element. type=C3D8R
   1.  212.  214.   18.   17.  856.  858.  244.  243
   2.  214.  207.   19.   18.  858.  851.  245.  244
   3.  210.  211.  214.  212.  854.  855.  858.  856
   4.  211.  208.  207.  214.  855.  852.  851.  858
   5.  211.  215.  209.  208.  855.  859.  853.  852
         ...
         ...
1348.  809. 1633. 1634.  810.  168.  830.  831.  167
1349.  810. 1634. 1621.  811.  167.  831.  818.   13
1350. 1631.  807.  806. 1630.  828.  170.  171.  827
1351. 1630.  806.  805. 1629.  827.  171.  172.  826
1352. 1629.  805.  804. 1622.  826.  172.  173.  819
** Region: (Bolt:Picked)
*Elset. elset=_11. internal. generate
      1.  1352.        1
** Section: Bolt
*Solid Section. elset=_11. material=HighSteel
1.,
*Node
    1635.              0.,              0.,              0.
*Nset. nset=_Preload_blrn_. internal
1635.
*End Instance
**
*Instance. name=Fl_Up-1. part=Fl_Up
*Node
        1.              0.,          0.013.           0.019
        2.              0.,             0.,           0.019
        3.         -0.013.              0.,           0.019
        4.              0.,             0.,              0.
        5.              0.,          0.013.              0.
         ...
         ...
 2356.    0.00265103.    0.00946248.    0.00633333
```

```
    2357.    0.00309956.    0.00775312.    0.00633333
    2358.    0.00353643.    0.00592631.    0.00633333
    2359.    0.00389121.    0.00400858.    0.00633333
    2360.    0.00414808.     0.0020239.    0.00633333
*Element. type=C3D8R
 1. 357. 34. 343. 1450. 21. 1. 33. 331
 2. 1450. 343. 344. 1449. 331. 33. 32.332
 3. 369. 370. 1457. 1455. 37. 36. 334. 333
 4. 370. 38. 358. 1457. 36. 2. 26. 334
 5. 1455. 1457. 1458. 1454. 333. 334. 336. 335
        ...
        ...
1698. 215. 329. 328. 214. 1086. 1447. 1446. 1087
1699. 214. 328. 327. 213. 1087. 1446. 1445. 1088
1700. 213. 327. 326. 212. 1088. 1445. 1444. 1089
1701. 324. 210. 211. 325. 1442. 1091. 1090. 1443
1702. 325. 211. 212. 326. 1443. 1090. 1089. 1444
** Region: (Flange:Picked)
*Elset. elset=_I1. internal. generate
1. 1702. 1
** Section: Flange
*Solid Section. elset=_I1. material=Steel
1.,
*End Instance
**
*Instance. name=loadcell-1. part=loadcell
0.001. 0.06. -0.019
0.001. 0.06. -0.019. 0.708107. -0.647107. -0.019. 180.
*Node
        1.      -0.0085.          0.,          0.
        2.       -0.012.          0.,          0.
        3.        0.012.          0.,          0.
        4.       0.0085.          0.,          0.
        5.       -0.012.          0.,        0.025
        ...
        ...
```

```
   176.     -0.0145623.     -0.0105801.          0.015
     177.      0.0145623.     -0.0105801.          0.02
     178.     0.00556231.      -0.017119.          0.02
     179.    -0.00556231.      -0.017119.          0.02
     180.     -0.0145623.     -0.0105801.          0.02
*Element, type=C3D8R
 1, 36, 41, 101, 85, 1, 2, 13, 20
 2, 85, 101, 102, 86, 20, 13, 14, 19
 3, 86, 102, 103, 87, 19, 14, 15, 18
 4, 87, 103, 104, 88, 18, 15, 16, 17
 5, 88, 104, 40, 29, 17, 16, 3, 4
          ...
          ...
 96, 6, 12, 84, 76, 37, 57, 177, 148
 97, 76, 84, 83, 75, 148, 177, 178, 147
 98, 75, 83, 82, 74, 147, 178, 179, 146
 99, 74, 82, 81, 73, 146, 179, 180, 145
100, 73, 81, 11, 5, 145, 180, 56, 44
** Region: (loadcell:Picked)
*Elset, elset=_I1, internal, generate
   1, 100, 1
** Section: loadcell
*Solid Section, elset=_I1, material=Loadcell
1.,
*End Instance
**
*Instance, name=Fl_Dn-1, part=Fl_Dn
4.0333e-18, 1.54108e-17, -1.02634e-48
4.0333e-18, 1.54108e-17, -1.02634e-48, -5.7199e-17, 1., 2.08899e-17, 180.
*Node
        1.          0.,       0.013,       0.019
        2.          0.,          0.,       0.019
        3.      -0.013.          0.,       0.019
        4.          0.,          0.,          0.
        5.          0.,       0.013.          0.
         ...
```

```
...
2202.      0.00287151.      0.00849832.          0.0095
2203.      0.00331509.      0.00692697.          0.0095
2204.      0.00369527.      0.00527337.          0.0095
2205.      0.00398553.      0.00355648.          0.0095
2206.      0.00418859.      0.00179212.          0.0095
*Element, type=C3D8R
1, 378, 379, 1421, 1420, 24, 23, 361, 360
2, 379, 36, 372, 1421, 23, 1, 35, 361
3, 385, 39, 380, 1426, 37, 2, 29, 362
4, 1426, 380, 381, 1425, 362, 29, 28, 363
5, 1425, 381, 382, 1424, 363, 28, 27, 364
...
...
1565, 353, 184, 185, 352, 1413, 791, 790, 1412
1566, 352, 185, 186, 351, 1412, 790, 789, 1411
1567, 351, 186, 187, 350, 1411, 789, 788, 1410
1568, 350, 187, 12, 349, 1410, 788, 787, 1409
1569, 184, 353, 354, 183, 791, 1413, 1414, 792
** Region: (Flange:Picked)
*Elset, elset=_I1, internal, generate
1,  1569,  1
** Section: Flange
*Solid Section, elset=_I1, material=Steel
1.,
*End Instance
*Nset, nset=_G42, internal, instance=Bolt-1
3,
*Nset, nset=_G43, internal, instance=loadcell-1
4,
*Nset, nset=_G96, internal, instance=Fl_Up-1
2,
*Nset, nset=_G109, internal, instance=Fl_Up-1
2, 3, 4, 6, 8, 9, 10, 12, 13, 15, 16, 17, 18, 36, 37, 38
39, 40, 41, 48, 49, 81, 82, 83, 84, 85, 86, 87, 88, 89, 90, 91
92, 93, 94, 95, 96, 97, 98, 99, 100, 101, 102, 103, 104, 105, 106, 107
```

108, 109, 110, 111, 112, 113, 114, 115, 116, 117, 118, 119, 120, 121, 122, 123
124, 125, 126, 127, 128, 142, 143, 151, 152, 153, 154, 155, 156, 157, 158, 159
160, 180, 181, 182, 183, 184, 185, 186, 187, 188, 189, 203, 204, 205, 206, 207
208, 229, 230, 231, 232, 233, 234, 235, 236, 237, 238, 258, 259, 260, 261, 262
263, 264, 265, 266, 267, 268, 269, 270, 271, 272, 273, 274, 275, 276, 277, 278
279, 280, 281, 282, 283, 284, 285, 286, 287, 288, 289, 290, 291, 292, 293, 301
302, 303, 304, 369, 370, 371, 372, 697, 698, 699, 700, 701, 702, 703, 704, 705
706, 707, 708, 709, 710, 711, 712, 713, 714, 715, 716, 717, 718, 719, 720, 721
722, 723, 724, 725, 726, 727, 728, 729, 730, 731, 732, 733, 734, 735, 736, 737
738, 739, 740, 741, 742, 743, 744, 1045, 1046, 1047, 1048, 1049, 1050, 1051, 1052, 1053
1054, 1055, 1056, 1057, 1058, 1059, 1060, 1061, 1062, 1063, 1064, 1145, 1146, 1147, 1148, 1149
1150, 1151, 1152, 1153, 1154, 1155, 1156, 1157, 1158, 1159, 1160, 1161, 1162, 1163, 1164, 1177
1178, 1179, 1180, 1181, 1182, 1183, 1184, 1185, 1186, 1187, 1188, 1189, 1190, 1191, 1192, 1193
1194, 1195, 1196, 1197, 1198, 1199, 1200, 1201, 1202, 1203, 1204, 1205, 1206, 1207, 1208, 1209
1210, 1211, 1212, 1213, 1214, 1215, 1216, 1217, 1218, 1219, 1220, 1221, 1222, 1223, 1224, 1405
1406, 1407, 1408
*Nset, nset=_G109, internal, instance=Fl_Dn-1
2, 3, 4, 6, 8, 9, 14, 15, 16, 17, 18, 19, 20, 37, 38, 39
40, 48, 49, 80, 81, 82, 83, 84, 85, 86, 87, 88, 89, 90, 91, 92
93, 94, 95, 96, 97, 98, 99, 100, 101, 102, 103, 104, 105, 106, 107, 108
109, 110, 111, 112, 113, 114, 115, 116, 117, 118, 119, 120, 121, 122, 123, 124
125, 126, 127, 141, 142, 211, 212, 213, 214, 215, 216, 217, 218, 219, 238, 239
240, 241, 242, 243, 244, 245, 246, 247, 248, 257, 258, 259, 260, 261, 262, 263
264, 283, 284, 285, 286, 287, 288, 289, 290, 291, 292, 293, 294, 295, 296, 297
298, 299, 300, 301, 302, 303, 304, 305, 306, 307, 308, 309, 310, 311, 312, 313
314, 315, 316, 317, 326, 327, 328, 329, 385, 386, 711, 712, 713, 714, 715, 716
717, 718, 719, 720, 721, 722, 723, 724, 725, 726, 727, 728, 729, 730, 731, 732
733, 734, 735, 736, 737, 738, 739, 740, 741, 742, 743, 744, 745, 746, 747, 748
749, 750, 751, 752, 753, 754, 755, 756, 757, 758, 1077, 1078, 1079, 1080, 1081, 1082
1083, 1084, 1111, 1112, 1113, 1114, 1115, 1116, 1117, 1118, 1119, 1134, 1135, 1136, 1137, 1138
1139, 1140, 1141, 1142, 1143, 1144, 1145, 1146, 1147, 1148, 1149, 1150, 1151, 1152, 1153, 1154
1155, 1156, 1157, 1158, 1159, 1160, 1161, 1162, 1163, 1164, 1165, 1166, 1167, 1168, 1169, 1170
1171, 1172, 1173, 1174, 1175, 1176, 1177, 1178, 1179, 1180, 1181, 1388, 1389
*Elset, elset=_G109, internal, instance=Fl_Up-1
3, 4, 20, 21, 22, 33, 34, 49, 50, 90, 96, 102, 108, 114, 120, 126
132, 138, 144, 150, 156, 162, 168, 174, 180, 186, 192, 198, 204, 210, 216, 222

228, 229, 235, 241, 247, 253, 259, 265, 271, 277, 283, 289, 295, 332, 338, 344
350, 356, 362, 368, 374, 380, 386, 392, 398, 404, 410, 416, 422, 428, 434, 440
446, 452, 458, 464, 470, 476, 482, 488, 494, 500, 506, 512, 518, 524, 530, 536
542, 548, 554, 560, 585, 589, 593, 597, 598, 610, 611, 612, 613, 614, 615, 697
698, 699, 700, 701, 725, 728, 731, 734, 737, 738, 765, 769, 773, 777, 778, 790
791, 792, 793, 794, 795, 877, 878, 879, 880, 881, 905, 908, 911, 914, 917, 918
945, 949, 953, 957, 958, 970, 971, 972, 973, 974, 975, 1057, 1058, 1059, 1060, 1061
1085, 1088, 1091, 1094, 1097, 1098, 1101, 1102, 1113, 1114, 1125, 1126, 1137, 1138, 1149, 1150
1161, 1162, 1173, 1174, 1185, 1186, 1197, 1198, 1209, 1210, 1221, 1222, 1233, 1234, 1274, 1280
1286, 1292, 1298, 1304, 1310, 1316, 1322, 1328, 1334, 1340, 1367, 1368, 1369, 1370, 1371, 1372
1373, 1374, 1375, 1376, 1377, 1378, 1379, 1445, 1446, 1447, 1448, 1449, 1450, 1451, 1452, 1453
1454, 1455, 1456, 1457, 1523, 1529, 1535, 1541, 1547, 1553, 1559, 1565, 1571, 1577, 1583, 1589
1595, 1606, 1612, 1615, 1626, 1632, 1638, 1644, 1649, 1650
*Elset, elset=_G109, internal, instance=Fl_Dn-1
3, 14, 20, 21, 29, 30, 70, 76, 82, 88, 94, 100, 106, 112, 118, 124
130, 136, 137, 138, 149, 150, 161, 162, 173, 174, 185, 186, 197, 198, 209, 210
221, 222, 233, 234, 245, 246, 257, 258, 269, 270, 312, 318, 324, 330, 336, 342
348, 354, 360, 366, 372, 378, 384, 390, 396, 402, 408, 414, 420, 426, 432, 438
444, 450, 456, 462, 468, 474, 480, 486, 492, 498, 504, 510, 516, 522, 528, 534
540, 608, 614, 620, 626, 632, 643, 649, 650, 671, 679, 690, 696, 697, 698, 725
729, 733, 740, 744, 780, 786, 792, 798, 804, 815, 821, 822, 843, 851, 862, 868
869, 870, 897, 901, 905, 912, 916, 917, 918, 931, 932, 945, 946, 959, 960, 973
974, 987, 988, 1001, 1002, 1015, 1016, 1029, 1030, 1043, 1044, 1057, 1058, 1071, 1072, 1115
1122, 1129, 1136, 1143, 1150, 1157, 1164, 1171, 1178, 1185, 1192, 1219, 1220, 1221, 1222, 1223
1224, 1225, 1226, 1227, 1228, 1229, 1230, 1231, 1310, 1311, 1312, 1313, 1314, 1315, 1316, 1317
1318, 1319, 1320, 1321, 1322, 1401, 1408, 1415, 1422, 1429, 1436, 1443, 1450, 1457, 1464, 1471
1478, 1485, 1498, 1505, 1508, 1521, 1528, 1531
*Nset, nset=Set_Monitor_Top, instance=Bolt-1
9, 10, 96, 97, 98, 99, 100, 101, 102, 103, 104, 105, 106, 107, 108, 109
134, 135, 136, 137, 138, 139, 443, 444, 445, 446, 447, 448, 449, 450, 451, 452
453, 454, 455, 456, 457, 458, 459, 460, 461, 462, 651, 652, 653, 654, 655, 656
657, 658, 659, 660, 661, 662, 663, 664, 665, 666, 667, 668, 669, 670
*Elset, elset=Set_Monitor_Top, instance=Bolt-1, generate
1095, 1148, 1
*Nset, nset=Set_Monitor_Bot, instance=Bolt-1
1, 2, 3, 4, 16, 17, 18, 19, 20, 21, 22, 23, 24, 25, 26, 27

28. 29. 30. 31. 32. 33. 110. 111. 112. 113. 114. 115. 116. 117. 118. 119
120. 121. 207. 208. 209. 210. 211. 212. 213. 214. 215. 216. 217. 218. 219. 220
519. 520. 521. 522. 523. 524. 525. 526. 527. 528. 529. 530. 531. 532
*Elset, elset=Set_Monitor_Bot, instance=Bolt-1
1. 2. 3. 4. 5. 6. 7. 8. 9. 10. 11. 12. 13. 14. 15. 16
17. 18. 19. 20. 21. 22. 23. 24. 25. 26. 27. 541. 542. 543. 544. 545
546. 547. 548. 549. 550. 551. 552. 553. 554. 555. 556. 557. 558. 559. 560. 561
562. 563. 564. 565. 566. 567
*Nset, nset=Set_Monitor_Mid, instance=Bolt-1
5. 6. 52. 53. 54. 55. 56. 57. 58. 59. 60. 61. 62. 63. 64. 65
122. 123. 124. 125. 126. 127. 221. 222. 223. 224. 225. 226. 227. 228. 229. 230
231. 232. 233. 234. 235. 236. 237. 238. 239. 240. 533. 534. 535. 536. 537. 538
539. 540. 541. 542. 543. 544. 545. 546. 547. 548. 549. 550. 551. 552
*Elset, elset=Set_Monitor_Mid, instance=Bolt-1
271. 272. 273. 274. 275. 276. 277. 278. 279. 280. 281. 282. 283. 284. 285. 286
287. 288. 289. 290. 291. 292. 293. 294. 295. 296. 297. 811. 812. 813. 814. 815
816. 817. 818. 819. 820. 821. 822. 823. 824. 825. 826. 827. 828. 829. 830. 831
832. 833. 834. 835. 836. 837
*Nset, nset=Set_RF_Monitor, instance=Bolt-1
5.
*Nset, nset=_G134, internal, instance=Bolt-1
5.
*Elset, elset=_Surf_Bt_Top_S1, internal, instance=Bolt-1, generate
1297, 1310, 1
*Surface, type=ELEMENT, name=Surf_Bt_Top
_Surf_Bt_Top_S1, S1
*Elset, elset=_Surf_Bt_Bot_S1, internal, instance=Bolt-1, generate
1081, 1094, 1
*Surface, type=ELEMENT, name=Surf_Bt_Bot
_Surf_Bt_Bot_S1, S1
*Elset, elset=_Surf_FlU_Bt_S1, internal, instance=Fl_Up-1, generate
1689, 1702, 1
*Surface, type=ELEMENT, name=Surf_FlU_Bt
_Surf_FlU_Bt_S1, S1
*Elset, elset=_Surf_FlU_Bot_S1, internal, instance=Fl_Up-1, generate
561, 740, 1

```
*Elset, elset=_Surf_FIU_Bot_S2, internal, instance=Fl_Up-1, generate
 1661,  1674,        1
*Elset, elset=_Surf_FIU_Bot_S3, internal, instance=Fl_Up-1
 1621, 1622, 1623, 1624, 1625, 1626, 1633, 1634, 1635, 1636, 1637, 1638, 1649, 1651, 1653, 1655
 1657, 1659
*Elset, elset=_Surf_FIU_Bot_S4, internal, instance=Fl_Up-1
 1646, 1648
*Surface, type=ELEMENT, name=Surf_FIU_Bot
_Surf_FIU_Bot_S1, S1
_Surf_FIU_Bot_S2, S2
_Surf_FIU_Bot_S4, S4
_Surf_FIU_Bot_S3, S3
*Elset, elset=_Surf_FID_Cell_S2, internal, instance=Fl_Dn-1
  541, 542, 543, 544, 545, 546, 547, 548, 549, 550, 551, 552, 553, 554, 555, 556
 1538, 1539, 1540, 1541, 1542, 1543, 1544, 1545, 1546, 1547, 1548, 1549, 1550, 1551, 1552, 1553
*Surface, type=ELEMENT, name=Surf_FID_Cell
_Surf_FID_Cell_S2, S2
*Elset, elset=_Surf_FID_Bot_S1, internal, instance=Fl_Dn-1
  557, 558, 559, 560, 561, 562, 563, 564, 565, 566, 567, 568, 569, 570, 571, 572
 1554, 1555, 1556, 1557, 1558, 1559, 1560, 1561, 1562, 1563, 1564, 1565, 1566, 1567, 1568, 1569
*Elset, elset=_Surf_FID_Bot_S2, internal, instance=Fl_Dn-1, generate
 745,  916,        1
*Elset, elset=_Surf_FID_Bot_S3, internal, instance=Fl_Dn-1
 1515, 1516, 1517, 1518, 1519, 1520, 1521, 1522, 1523, 1524, 1525, 1526, 1527, 1528, 1531, 1532
 1533, 1534, 1535, 1536, 1537
*Elset, elset=_Surf_FID_Bot_S4, internal, instance=Fl_Dn-1
 1529, 1530
*Surface, type=ELEMENT, name=Surf_FID_Bot
_Surf_FID_Bot_S1, S1
_Surf_FID_Bot_S2, S2
_Surf_FID_Bot_S4, S4
_Surf_FID_Bot_S3, S3
*Elset, elset=_Surf_Cell_Fl_S2, internal, instance=loadcell-1
  1, 2, 3, 4, 5, 26, 27, 28, 29, 30, 51, 52, 53, 54, 55, 76, 77, 78, 79, 80
*Surface, type=ELEMENT, name=Surf_Cell_Fl
_Surf_Cell_Fl_S2, S2
```

*Elset, elset=_Surf_Cell_Bt_S1, internal, instance=loadcell-1
21, 22, 23, 24, 25, 71, 72, 73, 74, 75
*Surface, type=ELEMENT, name=Surf_Cell_Bt
_Surf_Cell_Bt_S1, S1
*Elset, elset=__G111_S3, internal, instance=Fl_Up-1
327, 328, 329, 330, 331, 332, 405, 406, 407, 408, 409, 410, 1341, 1354
*Elset, elset=__G111_S3, internal, instance=Fl_Dn-1
307, 308, 309, 310, 311, 312, 1193, 1206
*Elset, elset=__G111_S4, internal, instance=Fl_Up-1
313, 326, 1379, 1392, 1405, 1418, 1431, 1444, 1457, 1470, 1483, 1496, 1509, 1522
*Elset, elset=__G111_S4, internal, instance=Fl_Dn-1
293, 306, 1231, 1244, 1257, 1270, 1283, 1296, 1309, 1322, 1335, 1348, 1361, 1374, 1387, 1400
*Elset, elset=__G111_S2, internal, instance=Fl_Up-1
483, 484, 485, 486, 487, 488, 1523, 1524, 1525, 1526, 1527, 1528
*Elset, elset=__G111_S2, internal, instance=Fl_Dn-1
385, 386, 387, 388, 389, 390, 391, 392, 393, 394, 395, 396, 1401, 1402, 1403, 1404, 1405, 1406, 1407
*Surface, type=ELEMENT, name=_G111, internal
__G111_S3, S3
__G111_S4, S4
__G111_S2, S2
*Elset, elset=__G131_S1, internal, instance=Bolt-1
406, 407, 408, 409, 410, 411, 412, 413, 414, 415, 416, 417, 418, 419, 420, 421
422, 423, 424, 425, 426, 427, 428, 429, 430, 431, 432, 946, 947, 948, 949, 950
951, 952, 953, 954, 955, 956, 957, 958, 959, 960, 961, 962, 963, 964, 965, 966
967, 968, 969, 970, 971, 972
*Surface, type=ELEMENT, name=_G131, internal
__G131_S1, S1
** Constraint: TIE_Cell_Bt
*Tie, name=TIE_Cell_Bt, adjust=yes
Surf_Cell_Bt, Surf_Bt_Bot
** Constraint: TIE_FlD_Cell
*Tie, name=TIE_FlD_Cell, adjust=yes
Surf_FlD_Cell, Surf_Cell_Fl
** Constraint: TIE_FlU_Bt
*Tie, name=TIE_FlU_Bt, adjust=yes
Surf_FlU_Bt, Surf_Bt_Top

```
** Pre-Tension Section for Bolt Load: Preload
*Pre-tension Section, surface= _G131, node=Bolt-1.1635
-1.15648e-15,    6.12323e-17,                    1.
*End Assembly
**
** MATERIALS
**
*Material, name=HighSteel
*Elastic
 3.175e+11, 0.3
*Plastic
 6.3627e+08,        0.
 8.382e+08, 0.0132
*Material, name=Loadcell
*Elastic
 2.13e+11, 0.3
*Material, name=Steel
*Elastic
 1.925e+11, 0.3
*Plastic
   3.8577e+08,          0.
 5.49096e+08, 0.0382
**
** INTERACTION PROPERTIES
**
*Surface Interaction, name=Fric
1.,
*Friction, rough
*Surface Interaction, name=Friction
1.,
*Friction, slip tolerance=0.005
 0.3,
**
** BOUNDARY CONDITIONS
**
** Name: Bolt_Fixed Type: Displacement/Rotation
```

```
*Boundary
_G42. 1. 1
_G42. 2. 2
_G42. 3. 3
** Name: Cell_Fixed Type: Displacement/Rotation
*Boundary
_G43. 1. 1
_G43. 2. 2
_G43. 3. 3
** Name: FIU_Fixed Type: Displacement/Rotation
*Boundary
_G96. 1. 1
_G96. 2. 2
_G96. 3. 3
** Name: FI_Sym Type: Symmetry/Antisymmetry/Encastre
*Boundary
_G109. YSYMM
**
** INTERACTIONS
**
** Interaction: FI_FI
*Contact Pair. interaction=Friction. small sliding. adjust=0.0
Surf_FID_Bot. Surf_FIU_Bot
** ----------------------------------------------------------------
**
** STEP: Preload
**
*Step. name=Preload
Preload 110KN
*Static
0.1. 1.. 1e-05. 1.
**
** BOUNDARY CONDITIONS
**
** Name: Bolt_Fixed Type: Displacement/Rotation
*Boundary. op=NEW
```

```
_G42. 1. 1
_G42. 2. 2
** Name: Cell_Fixed Type: Displacement/Rotation
*Boundary. op=NEW
_G43. 1. 1
_G43. 2. 2
** Name: FlU_Fixed Type: Displacement/Rotation
*Boundary. op=NEW
_G96. 1. 1
_G96. 2. 2
_G96. 3. 3
** Name: Fl_Sym Type: Symmetry/Antisymmetry/Encastre
*Boundary. op=NEW
_G109. YSYMM
**
** LOADS
**
** Name: Preload      Type: Bolt load
*Cload
Bolt-1._Preload_blrn_. 1. 110000.
**
** INTERACTIONS
**
** Interaction: Fl_Fl
*Contact Interference. shrink
Surf_FlD_Bot. Surf_FlU_Bot
**
** OUTPUT REQUESTS
**
*Restart. write. frequency=1
**
** FIELD OUTPUT: F-Output-1
**
*Output. field
*Node Output
U. RF
```

```
*Element Output
S, E
*Contact Output
CSTRESS,
**
** HISTORY OUTPUT: H-Output-1
**
*Output, history
*Node Output, nset=Set_RF_Monitor
RF3,
*El Print, freq=999999
*Node Print, freq=999999
*End Step
** ----------------------------------------------------------------
**
** STEP: Load
**
*Step, name=Load
Loading
*Static
0.1, 1., 1e-05, 1.
**
** BOUNDARY CONDITIONS
**
** Name: Monitor Type: Displacement/Rotation
*Boundary
_G134, 3, 3
**
** LOADS
**
** Name: Loading      Type: Pressure
*Dsload
_G111, P, -5.088e+08
**
** INTERACTIONS
**
```

```
** Interaction: FI_FI
*Contact Interference
Surf_FID_Bot, Surf_FIU_Bot, 0.,
**
** OUTPUT REQUESTS
**
*Restart, write, frequency=1
**
** FIELD OUTPUT: F-Output-1
**
*Output, field
*Node Output
U, RF
*Element Output
S, E
*Contact Output
CSTRESS,
**
** HISTORY OUTPUT: H-Output-1
**
*Output, history
*Node Output, nset=Set_RF_Monitor
RF3,
*End Step
```

APPENDIX E

(Sample Design)

Appendix E

Sample design

• Given: Design a bolted round bar connection under tensile load 120 kN and flange shape is assumed as circular.
(Material property: ASTM A572 – 50; σ_y = 345 MPa, σ_u = 450 MPa)

Design

- Rod diameter: $D \geq \sqrt{\frac{4T}{\sigma_y \pi}} = \sqrt{\frac{4 \times 120{,}000}{345 \times 10^6 \times \pi}} = 0.021$ m

so, D = 0.024 m (USE)

- Assume M20 (ASTM A325) * 2
- Hole diameter = 0.02 + 0.002 = 0.022 m
- Bolt pitch = p = 4.5 d = 4.5 * 0.02 = 0.09 m

so, a = 0.09 / 2 = 0.045 m (USE)

b >= a / 1.25 = 0.045 / 1.25 = 0.036 → 0.036 m (USE)

Therefore, radius of flange = a + b + D / 2 = 0.045 + 0.036 + 0.024 / 2 = 0.093 m

- $K = 4\,b'\,10^3 / (\Phi\, p\, F_y) = 4 * (36 - 20/2) * 10^3 / (0.9 * 90 * 345) = 3.721$
- $\delta = 1 - d'/p = 1 - 22/90 = 0.756$

$$t_{min} = \sqrt{\frac{KP_f}{(1+\delta)}} = \sqrt{\frac{3.721 \times (120/2)}{(1+0.756)}} = 11.28 \text{ mm}$$

$$t_{max} = \sqrt{KP_f} = \sqrt{3.721 \times (120/2)} = 14.94 \text{ mm}$$

so, t = 13.0 mm (USE)

Design check

1) Connection Capacity

- $T_n = \Phi_\beta\ 0.75\ A_b\sigma_u$ = 0.67 * 0.75 * 3.14 / 4 * 0.02 ^2 * 830 * 10^6 = 130.96 kN

$$-\alpha = \left(\frac{KT_r}{t^2} - 1\right) \times \frac{a'}{\delta(a'+b')} \quad , 0 \le \alpha \le 1.0$$

$$= \left(\frac{3.721 \times 130.96}{13^2} - 1\right) \times \frac{(45 + 20/2)}{0.756((45 + 20/2) + (35 - 20/2))}$$

= 1.712 → 1

- $C = (t^2/K)\,(1+\delta\alpha)\,n \ge$ Total load applied

= (13^2 / 3.721) * (1 + 0.756 * 1) * 2 = 159.50 kN >120 kN (OK)

2) Bolt Capacity

$$-\alpha = \left(\frac{KP_{fr}}{t^2} - 1\right) \times \frac{1}{\delta} = \left(\frac{3.721 \times (120/2)}{13^2} - 1\right) \times \frac{1}{0.756} = 0.424$$

$$-B = \left[1 + \frac{\delta\alpha}{(1+\delta\alpha)}\frac{b}{a}\right]T = \left[1 + \frac{0.756 \times 0.424}{(1 + 0.756 \times 0.424)}\frac{35}{45}\right] \times (120/2) = 71.33 \text{ kN}$$

$$-\sum_{i=1}^{n} B_i \ge \sum T \ : 71.33 \text{ kN} * 2 = 142.66 \text{ kN} > 120 \text{ kN} \quad \text{(OK)}$$

$$-T_r \ge B \ : 130.96 \text{ kN} > 71.33 \text{ kN} \quad \text{(OK)}$$

APPENDIX F

(Source Code for Design Program)

```
% APPENDIX F
% flange.m
%
% Programmed by yail J. Kim
% July 5 2002
%
T=input('Total load applied?(KN)');
Fy=input('Yield Strength of Flange(MPa)?');
Fu=input('Ultimate strength of Flange(MPa)?');
n=input('Number of bolts?');
m=menu('Select Bolt Size:','M20','M22','M24')


Dr=sqrt( 4 * T * 10^3 / ( Fy * 10^6 * 3.14 )) * 1.2 * 1000      %F.S = 1.2

        if m==1

                d = 20
                dh = d + 2
                p = 4.5 * d
                a = p / 2
                b = a / 1.25

        elseif m==2

                d = 22
                dh = d + 2
                p = 4.5 * d
                a = p / 2
                b = a / 1.25

        else

                d = 24
                dh = d + 2
                p = 4.5 * d
```

```
                a = p / 2
                b = a / 1.25

end

%% K = 4 * b' * 10^3 / ( pi * p * Fy )

        K = 4 * (( b - d / 2 )) * 10^3 / (0.9 * p * Fy)


m=menu('Select Bolt Property:','A325','A490')

if m==1
        Su = 830            %% Su =   Ultimate Strength of Bolt: 830MPa for A325

else
        Su = 1040           %% Su = Ultimate Strength of Bolt:1040MPa for A490

end

%% Tr = pi_b * 0.75 * Ab * Su

        Tr = 0.67 * 0.75 * 3.14 / 4 * (d/1000)^2 * (Su*10^6) / 1000

%% del = 1 - d' / p     :   d' = hole diameter all dimensions are mm.

        del = 1 - ( dh / p )

%% t_min = sqrt( K * (T/n) / ( 1 + del ))

        t_min = sqrt( K * ( T / n ) / ( 1 + del ) )

%% t_max = sqrt( K * (T/n) )

        t_max = sqrt( K * ( T / n ) )
```

```
%% t_used = ( t_max + t_min )/ 2

        t_used = ( t_max + t_min ) / 2

%%
%% Design Check-up
%%

%% 1) Connection Capacity Check-up

        %% alpha = ( K * Tr / ( t_used^2 )   - 1 ) * ( a' / ( del * ( a' + b' )))

                alpha = ( K * Tr / ( t_used^2) - 1 ) * ( ( a + d / 2 ) / ( del * ( a + d / 2 ) + ( b - d /
2 )))

                        if alpha > 1

                                alpha = 1

                                disp('alpha is modified since bigger than 1')

                        end


        %% Connection Capacity = ( t^2 / K ) * ( 1 + del * alpha ) * n >= Total applied load

                C = ( t_used^2 / K ) * ( 1 + del * alpha ) * n

                        if C >= T

                                disp ('Connection Capacity = OK' )

                        else

                                disp ( 'assume bolt size again' )
```

```
                    end

%% 2) Bolt Capacity Check-up

        %% alpha1 = ( K * ( T / n ) / ( t_used^2 ) - 1 ) * 1 / del

                alpha1 = ( K * ( T / n ) / ( t_used^2) -1 ) * 1 / del

        %% Bolt Capacity = [ 1 + del * alpha1 / ( 1 + del * alpha1 ) * b / a ] * ( T / n )


                B = ( 1 + del * alpha1 / ( 1 + del * alpha1 ) * b / a ) * ( T / n )

                    if B <= Tr

                            disp ('Bolt Capacity = OK' )

                    else

                            disp ( 'assume bolt size again' )

                    end


fprintf('Diameter of rod:%.3f(mm)',Dr);
fprintf('a:%.3f(mm)',a);
fprintf('b:%.3f(mm)',b);
fprintf('t_used:%.3f(mm)',t_used)
```

APPENDIX G

(Photographs)

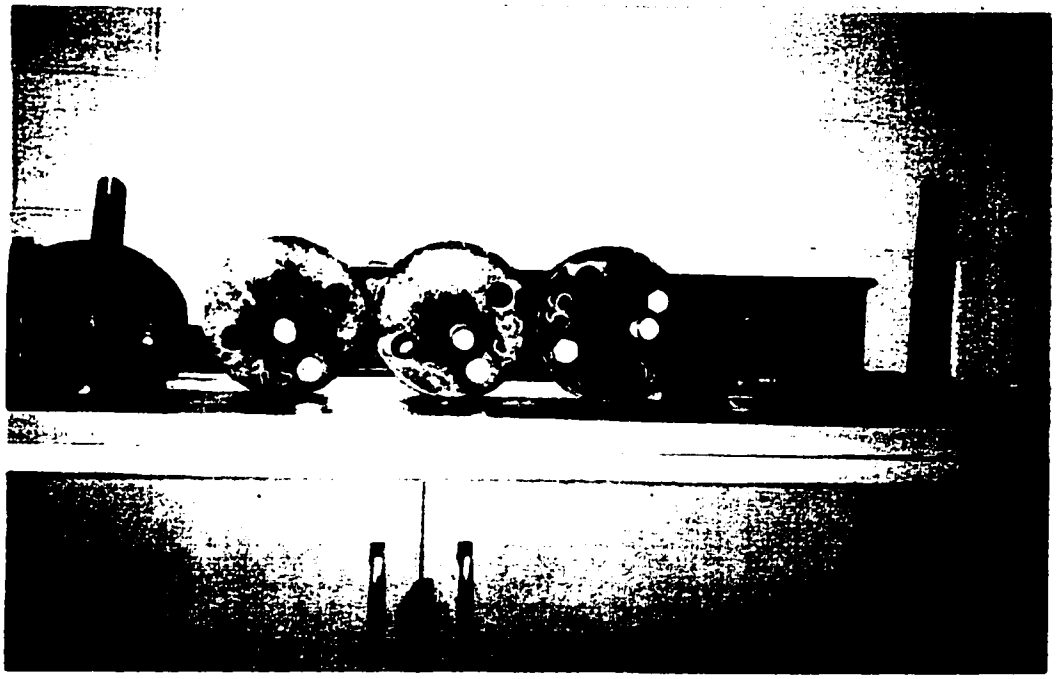

[Photo 1 - Specimens]

[Photo 2 - Broken specimens]

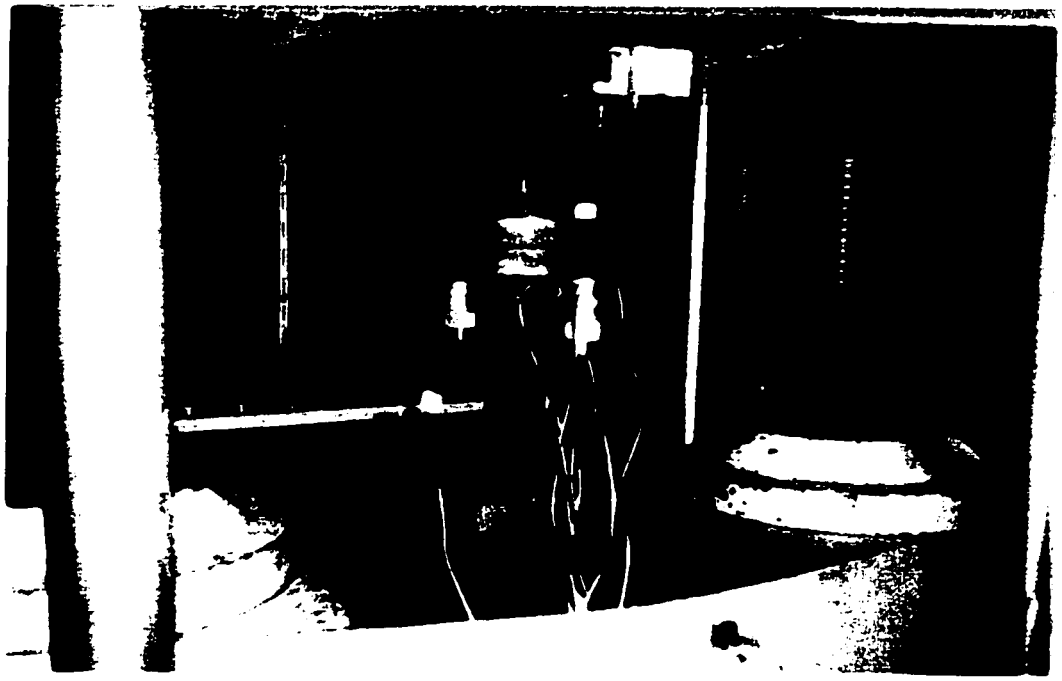

[Photo 3 - Testing with a load cell (S-1)]

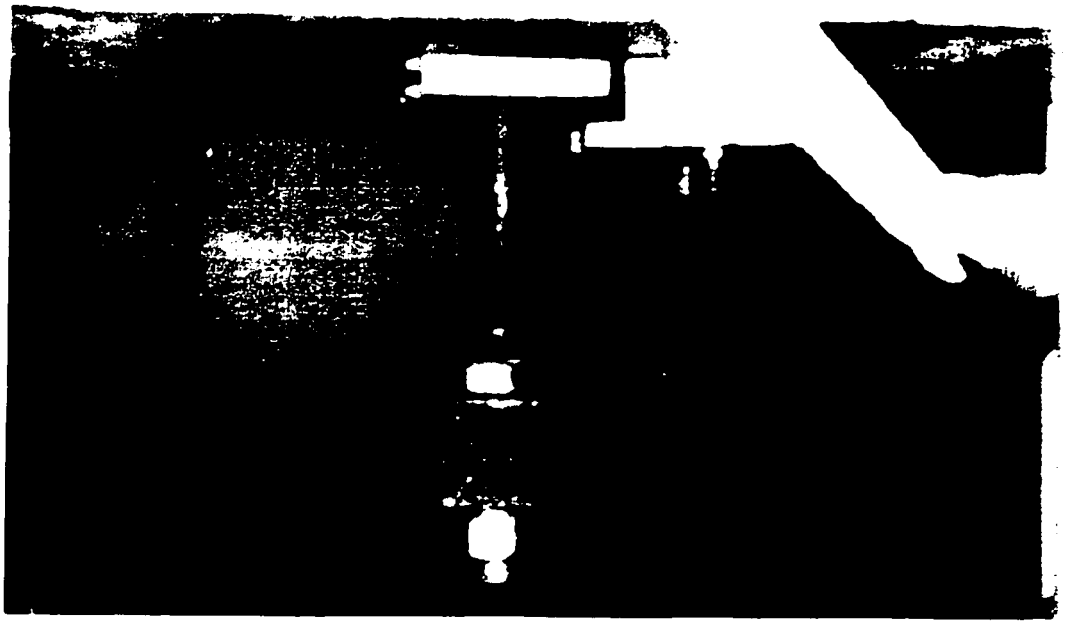

[Photo 4 - Necking]

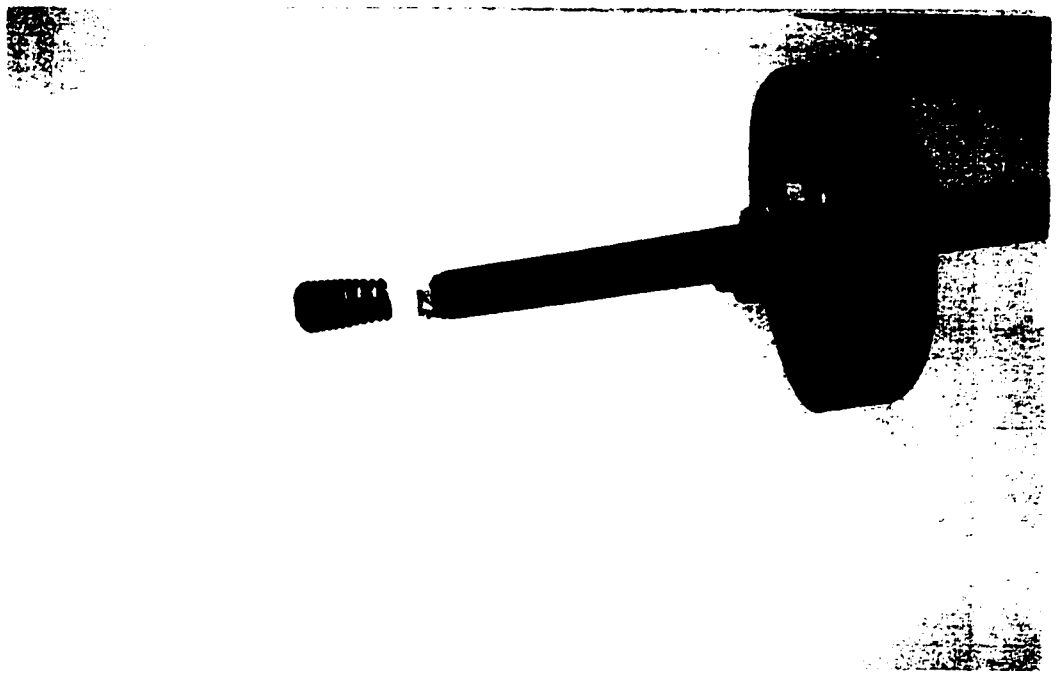

[Photo 5 - Broken threads (S-6)]

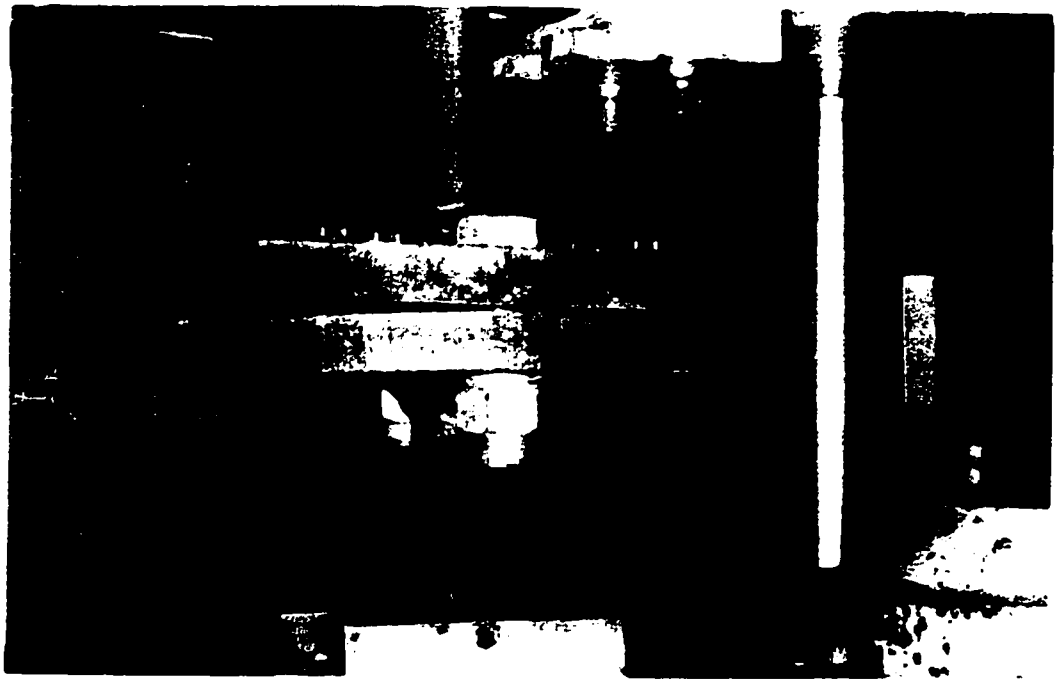

[Photo 6 - Asymmetric separation]

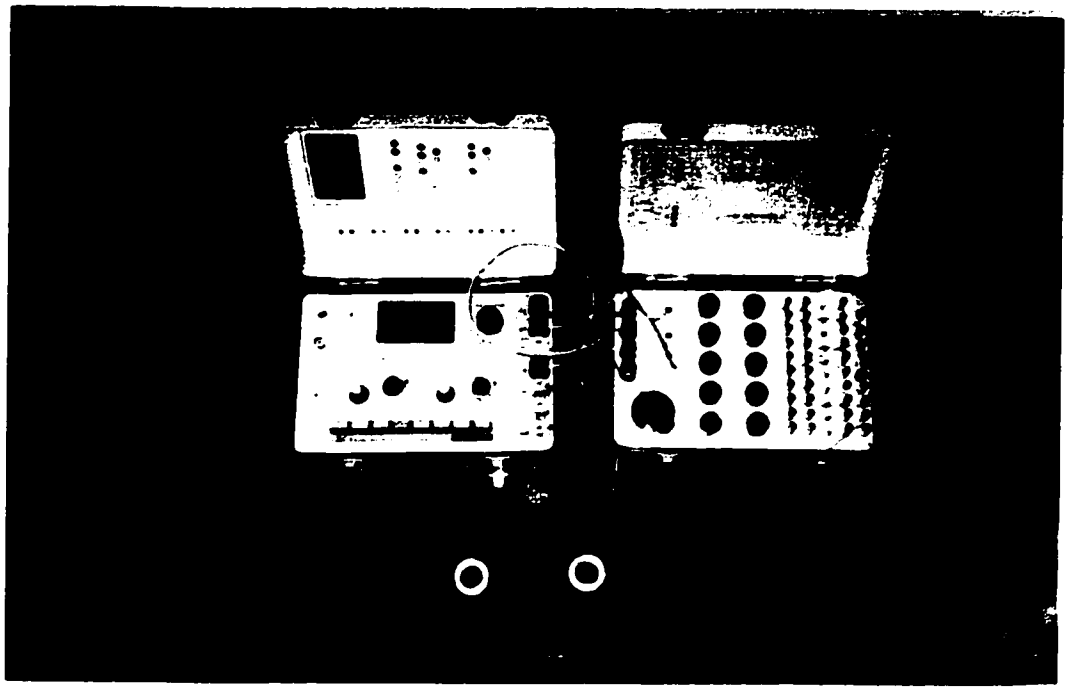

[Photo 7-Strain gages]

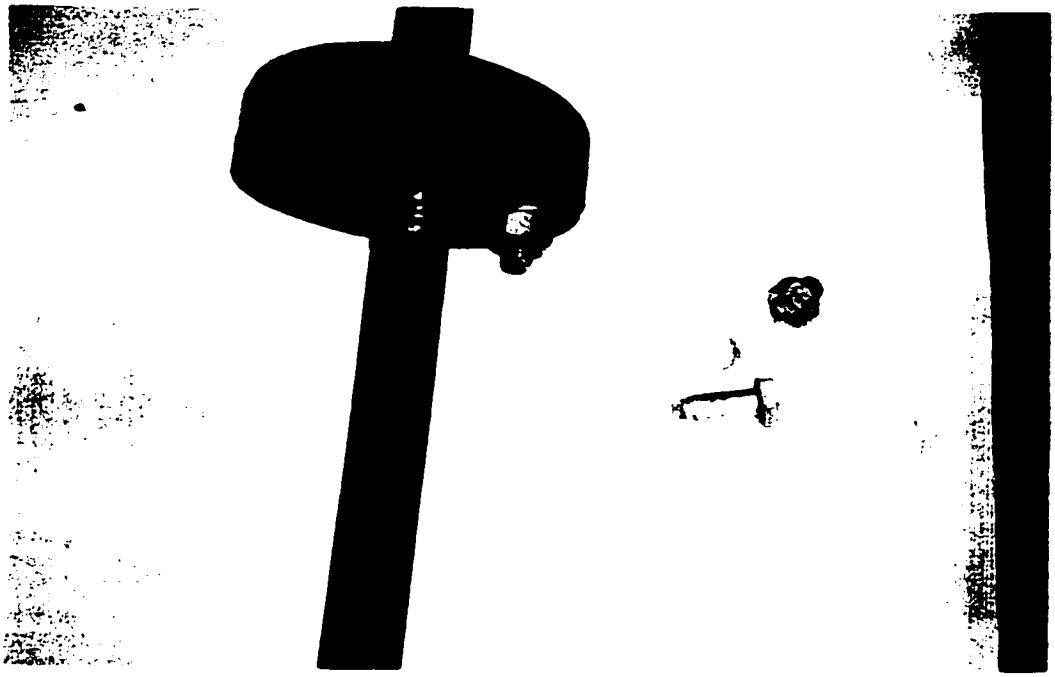

[Photo 8 - Broken specimen (F-1)]

Vita Auctoris

Legal Name: yail Kim

D.O.B: June 18, 1971

Engineering Motto

This can lead to a blind reliance on formulas, with a resulting lack of actual understanding

Educational Background

University of Windsor, Windsor, ON, Canada (2001 May ~ Present)

Expected to receive M. A. Sc majoring in Structural Engineering

Department of Civil & Environmental Engineering, Oct. 2002

Dongguk University, Seoul, S. Korea (1990 Mar. ~ 1994.Feb)

B. Eng in Civil Engineering,

Department of Civil & Environmental Engineering, Feb. 1994

Certificate

N.T.Q.C. (National Technical Qualification Certificate (1^{st} class) in Civil Engineering)

by Korea Man-Power Agency, Seoul S. Korea, 1993.

C.E.C.M. (Certificate of Education as a Construction Manager)

by Construction Industrial Education Center, Seoul S. Korea, 1998.

Membership

Member, K.S.C.E (Korean Society of Civil Engineer)

Member, K.O.C.E.A.(Korean Construction Engineer Association)

Professional Experience

University of Windsor – Graduate Assistant (May 2001~present)

Global Language Institute –English Instructor (May 2000 ~ Feb. 2001)

Bo-sung Const. and Eng. Co. Ltd – Construction Manager (Apr. 1999 ~ Oct. 1999)

Se-shin Engineering Co. Ltd –Construction Manager (Feb. 1998 ~ Mar. 1999)

Doo-San Engineering Co. Ltd. – Bridge Designer (Mar. 1997 ~ Jan. 1998)

Central Construction Co. Ltd. –Civil Engineer (Dec. 1993 ~ Feb. 1997)